Table 1 **Demographic characteristics of 147 subjects according to the presence of NPs or NFTs[a]**

Variables	Without NPs (CERAD = 0) (n = 47)	With NPs (CERAD = 1 to 3) (n = 100)	Without NFTs (Braak stage = 0) (n = 19)	With NFTs (Braak stage = I to VI) (n = 127)
Male sex, %	41.9	46.5	51.3	43.9
Age at medical examination, y	63 ± 1	71 ± 1[b]	62 ± 2	69 ± 1[b]
Fasting plasma glucose, mmol/L	5.7 ± 0.2	6.0 ± 0.1	5.6 ± 0.3	5.9 ± 0.1
Fasting insulin, μU/mL	4.5 (4.0, 5.2)	5.5 (5.0, 6.0)[b]	5.1 (4.1, 6.2)	5.2 (4.8, 5.6)
Systolic blood pressure, mm Hg	143.3 ± 3.6	137.5 ± 2.4	135.4 ± 5.7	139.8 ± 2.1
Diastolic blood pressure, mm Hg	78.1 ± 1.9	76.0 ± 1.3	76.4 ± 2.9	76.5 ± 1.1
TC, mmol/L	4.9 ± 0.2	5.4 ± 0.1[b]	5.5 ± 0.3	5.2 ± 0.1
LDLC, mmol/L	3.0 ± 0.2	3.6 ± 0.1[b]	3.8 ± 0.2	3.4 ± 0.1
HDLC, mmol/L	1.4 ± 0.1	1.3 ± 0.03	1.3 ± 0.1	1.3 ± 0.0
TG, mmol/L	1.0 (0.9, 1.2)	1.2 (1.1, 1.3)	1.1 (0.9, 1.4)	1.1 (1.0, 1.2)
TC/HDLC	3.7 ± 0.2	4.6 ± 0.1[b]	4.5 ± 0.3	4.3 ± 0.1
LDLC/HDLC	2.4 ± 0.2	3.0 ± 0.1[b]	3.0 ± 0.3	2.8 ± 0.1
Non-HDLC, mmol/L	3.5 ± 0.2	4.2 ± 0.1[b]	4.2 ± 0.3	3.9 ± 0.1
Body mass index, kg/m^2	21.8 ± 0.5	21.9 ± 0.3	21.6 ± 0.7	21.9 ± 0.3
Current smoking, %	49.5	43.6	59.4	40.3
Regular exercise, %	6.6	5.2	0.2	8.6
APOE ε4 carrier, %	0.03	21.8[b]	17.6	14.5

Abbreviations: CERAD = Consortium to Establish a Registry for Alzheimer's Disease; HDLC = high-density lipoprotein cholesterol; LDLC = low-density lipoprotein cholesterol; NFT = neurofibrillary tangle; NP = neuritic plaque; TC = total cholesterol; TG = triglycerides.
[a] Values are %, mean ± SE, or geometric mean (95% prediction interval). Geometric means of fasting insulin and triglycerides are shown due to the skewed distribution. Values are adjusted for age and sex except for sex and age at medical examination.
[b] $p < 0.05$. Male sex is adjusted for age. Age at medical examination is adjusted for sex.

was 59.2% (n = 87), which included any type of infarction (n = 73), hemorrhage (n = 10), or Binswanger type change (n = 6).

As shown in tables 2 and 3, we compared adjusted mean or geometric mean values of each lipid profile among groups according to CERAD score for NPs or Braak stage for NFTs. In the age- and sex-adjusted analyses (model 1), the subjects with NPs (CERAD score 1 to 3) showed significantly higher TC, LDLC, TC/HDLC, LDLC/HDLC, and non-HDLC levels compared to subjects without NPs (CERAD score 0). These associations remained significant even after multivariate model analysis (model 2 and 3). Test for trend among 4 CERAD stages revealed a limited dose-response relationship after multivariate model analysis. Unfavorable lipid metabolism was significantly associated with plaque-type AD pathology even in sparse to moderate stages (CERAD = 1 or 2). In contrast, we found no significant association between any lipid profile and NFT pathology (Braak stage I to VI vs stage 0).

To confirm these associations, we compared the risk of NPs among quartiles of each lipid profile in table 4. Compared with the lowest quartile (Q1) of TC, age- and sex-adjusted risks of NPs (model 1) were constant in the second (Q2) and the third (Q3) quartiles, but were significantly increased in the highest quartile (Q4). This relationship remained significant even after multivariate adjustment (model 2). Further adjustment for *APOE* genotype resulted in a higher increased risk of NPs (model 3). In a similar way, the highest quartiles of LDLC, TC/HDLC, LDLC/HDLC, and non-HDLC showed increased risk for NPs compared with the lowest respective quartiles. These findings suggested that the relationship between lipid profiles and the presence of NPs may fit with threshold models but not with linear models.

Additionally, table 4 shows ORs for the presence of NPs relative to lipid profile levels, namely low or high. We set the threshold level between Q3 and Q4 (lipid profiles excluding HDLC) or between Q1 and Q2 (HDLC). NPs were found in 86.1% of subjects with high TC (>5.80 mmol/L) and in 62.2% of people with low TC (≤5.80 mmol/L). Compared with low TC, the age- and sex-adjusted risk of NPs was significantly increased for high TC (model 1). After multivariate adjustments (models 2 and 3), this relationship remained significant. In a similar way, high levels of LDLC, TC/HDLC, LDLC/HDLC, and non-HDLC showed significantly increased risk for NPs compared with low levels, even after multivariate adjustments. When we performed similar analyses in which we narrow down the subjects with NPs to the group of CERAD = 2 to 3 (table e-1 on the *Neurology*® Web site at www.neurology.org) or CERAD = 3 (table e-2), similar associations between the lipid profiles and NPs were observed. The similar findings were observed even in the sensitivity analyses that excluded 26 cases with Alzheimer-type dementia (table e-3), or those that excluded 28 *APOE* ε4 carriers (data not shown). Because of the limited sample size, we could not perform sex-specific analyses.

DISCUSSION Using a series of autopsy cases from a general Japanese population, we found that high levels of TC, LDLC, TC/HDLC, LDLC/HDLC, and non-HDLC were significantly associated with plaque-type AD pathology. Our findings also suggest that the relationship between these lipid profiles and NPs may have certain threshold levels.

Because lipid metabolism is closely related to *APOE* genotype,[15] which is a strong risk factor for AD pathogenesis,[16] we compared the results of 2 multivariate models (model 2 and 3). The relationship between HDLC levels and the risk of NPs was diminished after adjustment for *APOE* genotype,

Table 2 Adjusted mean or geometric mean values of each lipid profile according to CERAD score[a]

	Model 1						Model 2						Model 3					
	CERAD score						CERAD score						CERAD score					
	0 (n = 47)	1 (n = 23)	2 (n = 22)	3 (n = 55)	p for trend	p (1–3 vs 0)	0 (n = 47)	1 (n = 23)	2 (n = 22)	3 (n = 55)	p for trend	p (1–3 vs 0)	0 (n = 47)	1 (n = 23)	2 (n = 22)	3 (n = 55)	p for trend	p (1–3 vs 0)
TC, mmol/L	4.87	5.47[b]	5.66[b]	5.32	0.07	0.006	4.85	5.47[b]	5.70[b]	5.34[b]	0.05	0.005	4.82	5.42[b]	5.69[b]	5.36	0.049	0.005
LDLC, mmol/L	3.05	3.54	3.83[b]	3.46	0.07	0.008	3.02	3.55	3.86[b]	3.47[b]	0.05	0.005	3.01	3.53	3.85[b]	3.50	0.05	0.007
HDLC, mmol/L	1.36	1.25	1.33	1.23	0.08	0.09	1.35	1.29	1.33	1.22	0.11	0.20	1.31	1.26	1.33	1.26	0.62	0.63
TG, mmol/L	1.00	1.30	0.99	1.22	0.20	0.09	1.02	1.25	1.00	1.22	0.25	0.18	1.06	1.25	1.01	1.15	0.77	0.49
TC/HDLC	3.73	4.64[b]	4.47[b]	4.56[b]	0.006	0.001	3.76	4.51[b]	4.50[b]	4.59[b]	0.004	0.001	3.87	4.58[b]	4.51	4.50[b]	0.05	0.009
LDLC/HDLC	2.39	2.93[b]	3.06[b]	2.96[b]	0.01	0.003	2.38	2.87	3.07[b]	2.99[b]	0.008	0.003	2.45	2.92	3.07[b]	2.94	0.06	0.02
Non-HDLC, mmol/L	3.51	4.21[b]	4.33[b]	4.10[b]	0.02	0.001	3.50	4.18[b]	4.37[b]	4.12[b]	0.01	0.001	3.51	4.16[b]	4.36[b]	4.10[b]	0.03	0.002

Abbreviations: CERAD = Consortium to Establish a Registry for Alzheimer's Disease; HDLC = high-density lipoprotein cholesterol; LDLC = low-density lipoprotein cholesterol; TC = total cholesterol; TG = triglycerides.

[a] Model 1 was adjusted for age and sex. Model 2 was adjusted for age, sex, systolic blood pressure, fasting blood glucose, fasting insulin, body mass index, current smoking, regular exercise, and cerebrovascular disease. Model 3 was adjusted for age, sex, systolic blood pressure, fasting blood glucose, fasting insulin, body mass index, current smoking, regular exercise, cerebrovascular disease, and APOE ε4 carrier. Geometric mean of triglyceride is shown due to the skewed distribution.

[b] $p < 0.05$ vs CERAD score = 0.

which suggested that *APOE* genotype was a confounding factor that had distorted the relationship between HDLC and NPs. Meanwhile, adjustment for *APOE* genotype resulted in a greater increased risk of NPs in association with high levels of TC, LDLC, and non-HDLC. These findings indicated that lipid profiles, such as TC, LDLC, and non-HDLC, may be significant risk factors for NPs and that these relationships were independent from *APOE* genotype.

There was a limited dose-response relationship between the lipid profiles and CERAD score after multivariate model analysis, which might be diminished by an epidemiologic competing effect, indicating that subjects with very high lipid profiles at the clinical examination probably died earlier as a result of cardiovascular disease, for example. Moreover, there might be a threshold effect, indicating that serum cholesterol in excess of a certain threshold level would trigger the plaque formation even though the further development of AD pathology might be modified by different factors. To control the serum cholesterol below a threshold level would decrease the risk of plaque formation, which might contribute to the prevention of AD.

Our analyses using quartiles suggested possible threshold levels to be approximately 6 mmol/L for TC and 4 mmol/L for LDLC. TC/HDLC, LDLC/HDLC, and non-HDLC are primarily the indexes for prediction of coronary heart disease based on a linear relationship[17]; nevertheless, our results also showed certain threshold levels for these indexes. This suggests that the increased risk of NP formation is less associated with atherosclerotic vascular factors. Lipid profiles were measured in blood samples; however, peripheral lipid profiles could be quite different from cholesterol metabolism in the brain. There may be a homeostatic regulation of cholesterol across the blood–brain barrier, which might adopt a threshold in the periphery. It is difficult to further estimate exact threshold levels due to the limited sample size of this study. Further studies with a larger sample size are needed to determine this issue.

The absence of a consistent association between the lipid profiles and NFT pathology in the present study might be due to the relatively small sample size; nevertheless, NFT pathology was less associated with disturbed lipid metabolism than was the formation of NPs, and NFT pathology is considered to be a consequence of Aβ deposition in the amyloid cascade hypothesis.[18] Lipid profiles may act upstream of the cascade, and might trigger AD pathogenesis. This is similar to the relationship between diabetes-related factors and NP pathology that we have previously reported.[3] The dissociation with the NFT could be

Table 3 Adjusted mean or geometric mean values of each lipid profile according to Braak and Braak staging[a]

	Model 1					Model 2					Model 3				
	Braak stage					Braak stage					Braak stage				
	0 (n = 19)	I, II (n = 26)	III, IV (n = 64)	V, VI (n = 37)	p for trend	0 (n = 19)	I, II (n = 26)	III, IV (n = 64)	V, VI (n = 37)	p for trend	0 (n = 19)	I, II (n = 26)	III, IV (n = 64)	V, VI (n = 37)	p for trend
TC, mmol/L	5.44	5.08	5.17	5.43	0.78	5.46	5.03	5.19	5.43	0.82	5.49	5.07	5.17	5.42	0.92
p (I–VI vs 0)					0.38					0.33					0.32
LDLC, mmol/L	3.75	3.25	3.34	3.45	0.59	3.77	3.21	3.36	3.45	0.58	3.83	3.24	3.36	3.46	0.50
p (I–VI vs 0)					0.12					0.11					0.09
HDLC, mmol/L	1.28	1.29	1.28	1.31	0.80	1.28	1.29	1.27	1.33	0.64	1.25	1.30	1.26	1.34	0.47
p (I–VI vs 0)					0.87					0.88					0.62
TG, mmol/L	1.09	1.06	1.03	1.34	0.17	1.11	1.07	1.05	1.28	0.33	1.14	1.08	1.04	1.24	0.56
p (I–VI vs 0)					0.97					0.94					0.73
TC/HDLC	4.44	4.15	4.24	4.42	0.88	4.46	4.11	4.30	4.34	0.96	4.58	4.11	4.33	4.32	0.73
p (I–VI vs 0)					0.55					0.49					0.32
LDLC/HDLC	2.96	2.72	2.75	2.81	0.78	2.98	2.69	2.78	2.78	0.69	3.07	2.70	2.81	2.78	0.55
p (I–VI vs 0)					0.46					0.41					0.28
Non-HDLC, mmol/L	4.16	3.79	3.88	4.13	0.84	4.19	3.74	3.92	4.10	0.92	4.24	3.77	3.91	4.08	0.91
p (I–VI vs 0)					0.35					0.29					0.23

Abbreviations: HDLC = high-density lipoprotein cholesterol; LDLC = low-density lipoprotein cholesterol; TC = total cholesterol; TG = triglycerides.
[a] Model 1 was adjusted for age and sex. Model 2 was adjusted for age, sex, systolic blood pressure, fasting blood glucose, fasting insulin, body mass index, current smoking, regular exercise, and cerebrovascular disease. Model 3 was adjusted for age, sex, systolic blood pressure, fasting blood glucose, fasting insulin, body mass index, current smoking, regular exercise, cerebrovascular disease, and *APOE ε4* carrier. Geometric mean of triglycerides is shown due to the skewed distribution.

another example that plaques and NFT are driven by very different factors.

Cholesterol may be associated with levels of the amyloid-precursor-protein metabolite Aβ, although the effects of cholesterol on Aβ metabolism, amyloid fibrillogenesis, and toxicity are not well understood and the results reported so far are controversial.[19,20] Aβ, apoE, cholesterol, and cholesterol oxidase have been shown to colocalize in the core of fibrillary plaques in transgenic mice models of AD,[21,22] which suggests that cholesterol and apoE are involved in fibrillar plaque formation. Previous studies have also found that levels of serum cholesterol, especially in the form of LDLC in patients with AD, were significantly higher when compared to age-matched controls.[23] A change in membrane properties, including stiffness and fluidity, has been suggested to influence activities of membrane-bound proteins and enzymes, including secretases. The high cholesterol content in lipid rafts, membrane regions where these enzymes are located, facilitates the clustering of the β and γ secretases with their substrates into an optimum configuration, thereby promoting the undesirable pathogenic cleavage of amyloid precursor protein.[24]

There are few previous studies that have investigated the association between hypercholesterolemia and AD-related pathology.[6,7] Of these, the Honolulu-Asia Aging Study was a population-based study which reported that the constituents of HDLC may play a role in the formation of AD pathology. The discrepancy between these and our results may reflect differences in study design. One difference is in the observation period between the evaluation of cholesterolemia and autopsy. Because the observation period in our study was relatively long (10–15 years) compared with the Honolulu-Asia Aging Study (<8 years), our study design might reduce the possibility of reverse causality; the presence of AD might affect the lifestyle of the subjects and their lipid profiles. Another retrospective study shows that serum hypercholesterolemia may be a risk factor for the development of AD amyloid pathology.[6] This study was not population-based and the increased risk is observed only among subjects younger than 55 years of age; however, significant association between serum cholesterol and the development of amyloid pathology is consistent with our findings.

Meanwhile, the relationship between cholesterol levels and clinical manifestation of dementia is less clear.[25] Epidemiology studies show controversial findings; high cholesterol levels in midlife may increase risk for subsequent dementia and AD[26–29] or low cholesterol levels in late life have been predictive of subsequent dementia.[30] Differences in study designs, length of observational periods, analytical

Table 4 **Multivariate-adjusted ORs and 95% CIs for presence of NPs (CERAD score 1–3 vs 0) according to lipid profile levels[a]**

Quantiles of lipid profiles	Range	No. of subjects with NPs/total (%)	Model 1		Model 2		Model 3	
			OR (95% CI)	*p* Value	OR (95% CI)	*p* Value	OR (95% CI)	*p* Value
TC, mmol/L								
Q1	≤4.48	23/37 (62.2)						
Q2 (vs Q1)	>4.48 and ≤5.20	23/37 (62.2)	1.1 (0.4–3.1)	0.93	0.9 (0.3–2.9)	0.8302	1.1 (0.3–4.4)	0.93
Q3 (vs Q1)	>5.20 and ≤5.80	23/37 (62.2)	1.0 (0.3–3.1)	0.96	0.7 (0.2–2.6)	0.62	0.7 (0.2–3.1)	0.65
Q4 (vs Q1)	>5.80	31/36 (86.1)	6.8 (1.8–25.4)	0.005	8.2 (1.9–35.2)	0.004	23.1 (3.8–141.6)	0.0007
Q4 (vs Q1–3)			6.6 (2.1–20.5)	0.001	9.6 (2.7–34.1)	0.0005	24.8 (4.7–130.5)	0.0002
LDLC, mmol/L								
Q1	≤2.75	22/37 (59.5)						
Q2 (vs Q1)	>2.75 and ≤3.35	24/36 (66.7)	1.6 (0.5–5.2)	0.39	1.1 (0.3–3.9)	0.87	1.0 (0.2–4.0)	0.97
Q3 (vs Q1)	>3.35 and ≤4.02	23/37 (62.2)	1.2 (0.4–3.6)	0.75	1.1 (0.3–3.8)	0.86	1.5 (0.4–6.0)	0.61
Q4 (vs Q1)	>4.02	30/35 (85.7)	7.5 (1.9–29.0)	0.004	8.1 (1.9–34.0)	0.005	13.5 (2.5–73.1)	0.003
Q4 (vs Q1–3)			5.8 (1.8–18.4)	0.003	7.5 (2.2–25.3)	0.001	11.6 (2.7–49.4)	0.0009
HDLC, mmol/L								
Q4	>1.50	20/31 (64.5)						
Q3 (vs Q4)	>1.27 and ≤1.50	24/38 (63.2)	0.7 (0.2–2.1)	0.49	0.7 (0.2–2.5)	0.63	0.9 (0.2–3.8)	0.94
Q2 (vs Q4)	>1,04 and ≤1.27	25/41 (61.0)	0.9 (0.3–2.7)	0.86	1.0 (0.3–3.3)	0.94	1.0 (0.2–3.8)	0.95
Q1 (vs Q4)	≤1.04	31/37 (83.8)	3.2 (0.9–11.5)	0.07	2.8 (0.7–11.0)	0.15	1.7 (0.4–7.8)	0.49
Q1 (vs Q2–4)			3.8 (1.3–10.9)	0.01	3.1 (1.1–9.2)	0.04	1.8 (0.6–5.6)	0.34
TG, mmol/L								
Q1	≤0.81	26/38 (68.4)						
Q2 (vs Q1)	>0.81 and ≤1.11	25/36 (69.4)	0.9 (0.3–2.8)	0.88	1.0 (0.3–3.4)	>0.99	0.9 (0.2–3.3)	0.87
Q3 (vs Q1)	>1.11 and ≤1.56	22/38 (57.9)	0.5 (0.2–1.5)	0.21	0.5 (0.2–1.7)	0.28	0.6 (0.2–2.1)	0.40
Q4 (vs Q1)	>1.56	27/35 (77.1)	2.7 (0.8–8.9)	0.11	3.1 (0.8–12.4)	0.10	2.7 (0.6–12.2)	0.19
Q4 (vs Q1–3)			3.5 (1.2–9.6)	0.02	4.0 (1.3–12.8)	0.02	3.5 (1.0–12.3)	0.05
TC/HDLC								
Q1	≤3.32	21/37 (56.8)						
Q2 (vs Q1)	>3.32 and ≤4.09	23/37 (62.2)	1.1 (0.4–3.2)	0.86	1.4 (0.4–4.4)	0.62	1.2 (0.3–4.4)	0.77
Q3 (vs Q1)	>4.09 and ≤5.10	24/38 (63.2)	1.8 (0.6–5.5)	0.27	2.6 (0.7–9.2)	0.14	1.8 (0.4–7.7)	0.41
Q4 (vs Q1)	>5.10	32/35 (91.4)	13.0 (2.8–59.9)	0.001	18.1 (3.1–105.5)	0.001	19.7 (2.6–149.4)	0.004
Q4 (vs Q1–3)			9.7 (2.5–37.1)	0.0009	9.7 (2.3–40.1)	0.002	13.1 (2.5–68.6)	0.002
LDLC/HDLC								
Q1	≤2.00	24/38 (63.2)						
Q2 (vs Q1)	>2.00 and ≤2.64	23/35 (65.7)	1.1 (0.4–3.1)	0.90	1.0 (0.3–3.3)	>0.99	1.0 (0.3–3.5)	0.96
Q3 (vs Q1)	>2.64 and ≤3.48	21/37 (56.8)	1.1 (0.4–3.2)	0.92	1.3 (0.4–4.3)	0.68	1.2 (0.3–4.9)	0.75
Q4 (vs Q1)	>3.48	31/35 (88.6)	5.7 (1.4–23.0)	0.01	6.9 (1.4–32.7)	0.02	7.9 (1.2–50.5)	0.03
Q4 (vs Q1–3)			5.5 (1.7–18.1)	0.005	6.0 (1.7–21.8)	0.007	7.0 (1.5–32.0)	0.01
Non-HDLC, mmol/L								
Q1	≤3.29	23/38 (60.5)						
Q2 (vs Q1)	>3.29 and ≤3.86	24/37 (64.9)	1.0 (0.4–3.1)	0.94	0.9 (0.3–3.0)	0.82	0.7 (0.2–2.9)	0.65
Q3 (vs Q1)	>3.86 and ≤4.61	22/37 (59.5)	1.0 (0.4–3.1)	0.95	1.0 (0.3–3.3)	0.95	0.7 (0.2–2.9)	0.64
Q4 (vs Q1)	>4.61	31/35 (88.6)	8.5 (2.1–34.6)	0.003	10.1 (2.1–48.2)	0.004	13.1 (2.3–75.9)	0.004
Q4 (vs Q1–3)			8.2 (2.4–28.2)	0.0008	10.7 (2.8–40.5)	0.0005	16.5 (3.5–77.6)	0.0004

Abbreviations: CERAD = Consortium to Establish a Registry for Alzheimer's Disease; CI = confidence interval; HDLC = high-density lipoprotein cholesterol; LDLC = low-density lipoprotein cholesterol; NP = neuritic plaque; OR = odds ratio; TC = total cholesterol; TG = triglycerides.

[a] Model 1 was adjusted for age and sex. Model 2 was adjusted for age, sex, systolic blood pressure, fasting blood glucose, fasting insulin, body mass index, current smoking, cerebrovascular disease, and regular exercise. Model 3 was adjusted for age, sex, systolic blood pressure, fasting blood glucose, fasting insulin, body mass index, current smoking, regular exercise, cerebrovascular disease, and *APOE* ε4 carrier.

strategies, and the age at the occurrence of high cholesterol may influence observations.[31] Our study evaluated how cholesterol affects the neuropathologic process of AD; however, dyslipidemia might also affect mechanisms other than NP formation in the onset of dementia or AD, such as cell-membrane maintenance or synaptic function.

There are some limitations to our present study. First, the crude, semiquantitative evaluation of NPs (CERAD) and NFTs (Braak stage) could affect the results of the present study. Second, the medical history of dyslipidemia, such as disease duration, use of medication, and complications, were not considered in this study. Medication or change of lifestyle between the clinical examination and death might affect the lipid profiles during a follow-up period; therefore, the association between lipid profiles and AD pathology could be underestimated in this study.

Despite these limitations, our study has several strengths. The main advantage over other studies is the direct measurement of lipid profiles, such as TC, TG, and HDLC, more than a decade before subjects died. We included community-based subjects, who had detailed metabolic characterization at midlife based on comprehensive blood testing, and we systematically assessed AD pathology. Accordingly, the data included in this study are valuable for the examination of metabolic risk factors for AD pathology. In the Hisayama Study, both participation rate of clinical examinations and autopsy rate have remained at high levels. Therefore, our results could apply to other Japanese populations.

As part of the Hisayama Study, we have shown that dyslipidemia, in addition to insulin resistance, may be an independent risk factor for NP formation. Due to the long follow-up period, a number of other factors may have come into play. Nonetheless, our study clearly makes the point that lipid profiles may contribute directly or indirectly to plaque burden in the brain. Because a direct measurement of LDLC may be unreliable, and for the purpose of additional consideration of very low-density lipoprotein and intermediate density lipoprotein cholesterol, the values of non-HDLC might help to predict the development of NPs. Further studies are required to determine if there is a causal link between dyslipidemia and the development of NPs or other AD-related pathologies. In the future, adequate control of cholesterol, in addition to the control of diabetes, might contribute to a strategy for the prevention of AD.

AUTHOR CONTRIBUTIONS

Dr. Matsuzaki: drafting/revising the manuscript, study concept or design, analysis or interpretation of data, acquisition of data, statistical analysis. Dr. Sasaki: drafting/revising the manuscript, study concept or design, analysis or interpretation of data, acquisition of data, obtaining funding. Dr. Hata: drafting/revising the manuscript, analysis or interpretation of data, acquisition of data, statistical analysis. Dr. Hirakawa: analysis or interpretation of data, acquisition of data. Dr. Fujimi: analysis or interpretation of data, acquisition of data. Dr. Ninomiya: drafting/revising the manuscript, acquisition of data. Dr. Suzuki: drafting/revising the manuscript, analysis or interpretation of data, contribution of vital reagents/tools/patients, acquisition of data. Dr. Kanba: analysis or interpretation of data, study supervision. Dr. Kiyohara: drafting/revising the manuscript, study concept or design, analysis or interpretation of data, contribution of vital reagents/tools/patients, acquisition of data, study supervision, obtaining funding. Dr. Iwaki: drafting/revising the manuscript, study concept or design, analysis or interpretation of data, acquisition of data, study supervision, obtaining funding.

ACKNOWLEDGMENT

The authors thank S. Nagae and K. Sato for technical assistance.

DISCLOSURE

Dr. Matsuzaki reports no disclosures. Dr. Sasaki receives research support from Grant-in-Aid for Scientific Research (C) from Japan Society for the Promotion of Science and Grant-in-Aid for Scientists from the Ministry of Health, Labour and Welfare, Japan. Dr. Hata, Dr. Hirakawa, Dr. Fujimi, Dr. Ninomiya, and Dr. Suzuki report no disclosures. Dr. Kanba serves on a scientific advisory board for Astellas Pharma Inc.; serves/has served on editorial advisory boards for *Molecular Psychiatry*, the *Journal of Neuroscience and Psychiatry*, the *Asian Journal of Psychiatry*, and the *Asia Pacific Journal of Psychiatry*; has received speaker honoraria from Janssen, Shanghai Tsumura Pharmaceuticals Co., Ltd., Ajinomoto Co., Inc., Yoshitomi Pharmaceutical Industries, Ltd., Meiji Seika Pharma Co., Ltd, Kyowa-Hakko, Dainippon Sumitomo Pharma Co., Ltd., Organon Pharmaceuticals, Otsuka Pharmaceutical Co., Ltd., Astellas Pharma Inc., Eli Lilly and Company, GlaxoSmithKline, Pfizer Inc, Asahi Kasei Kuraray Medical Co., Ltd., and Shionogi & Co., Ltd.; has served as consultant for Eli Lilly and Company, GlaxoSmithKline, Pfizer Inc, Mitsubishi Tanabe Pharma Corporation, Ono Pharmaceutical Co. Ltd., Astellas Pharma Inc., Asahi-kasei, Shionogi, and Otsuka Pharmaceutical Co., Ltd.; and receives/has received research support from has received research support from Eli Lilly and Company, GlaxoSmithKline, Pfizer Inc, Asahi Kasei Kuraray Medical Co., Ltd., Janssen, Shanghai Tsumura Pharmaceuticals Co., Ltd., Ajinomoto Co., Inc., Yoshitomi Pharmaceutical Industries, Ltd., Meiji Seika Pharma Co., Ltd, Kyowa Hakko Kirin Pharma, Inc., Dainippon Sumitomo Pharma Co., Ltd., Organon Pharmaceuticals, Otsuka Pharmaceutical Co., Ltd., Ono Pharmaceutical Co. Ltd., and Japanese Ministry of Education and of Health. Dr. Kiyohara receives research support from a Health and Labour Sciences Research Grant of the Ministry of Health, Labour and Welfare, Japan. Dr. Iwaki serves as an Associate Editor for *Brain Tumor Pathology* and on the editorial boards of *Neuropathology*, *Pathology-Research and Practice*, and *Pathology International*; and receives research support from a Grant-in-Aid for Scientific Research (B) from Japan Society for the Promotion of Science (JSPS).

Received February 16, 2011. Accepted in final form May 23, 2011.

REFERENCES

1. Matsui Y, Tanizaki Y, Arima H, et al. Incidence and survival of dementia in a general population of Japanese elderly: the Hisayama Study. J Neurol Neurosurg Psychiatry 2009;80:366–370.
2. Sekita A, Ninomiya T, Tanizaki Y, et al. Trends in prevalence of Alzheimer's disease and vascular dementia in a Japanese community: the Hisayama Study. Acta Psychiatr Scand 2010;122:319–325.
3. Matsuzaki T, Sasaki K, Tanizaki Y, et al. Insulin resistance is associated with the pathology of Alzheimer disease: the Hisayama Study. Neurology 2010;75:764–770.
4. Peila R, Rodriguez BL, Launer LJ. Type 2 diabetes, APOE gene, and the risk for dementia and related pathologies:

The Honolulu-Asia Aging Study. Diabetes 2002;51:1256–1262.
5. Arvanitakis Z, Schneider JA, Wilson RS, et al. Diabetes is related to cerebral infarction but not to AD pathology in older persons. Neurology 2006;67:1960–1965.
6. Pappolla MA, Bryant-Thomas TK, Herbert D, et al. Mild hypercholesterolemia is an early risk factor for the development of Alzheimer amyloid pathology. Neurology 2003;61:199–205.
7. Launer LJ, White LR, Petrovitch H, Ross GW, Curb JD. Cholesterol and neuropathologic markers of AD: a population-based autopsy study. Neurology 2001;57:1447–1452.
8. Katsuki S. Epidemiological and clinicopathological study on cerebrovascular disease in Japan. Prog Brain Res 1966;21:64–89.
9. Ohmura T, Ueda K, Kiyohara Y, et al. Prevalence of type 2 (non-insulin-dependent) diabetes mellitus and impaired glucose tolerance in the Japanese general population: the Hisayama Study. Diabetologia 1993;36:1198–1203.
10. Fujimi K, Sasaki K, Noda K, et al. Clinicopathological outline of dementia with Lewy bodies applying the revised criteria: the Hisayama Study. Brain Pathol 2008;18:317–325.
11. Friedewald WT, Levy RI, Fredrickson DS. Estimation of the concentration of low-density lipoprotein cholesterol in plasma, without use of the preparative ultracentrifuge. Clin Chem 1972;18:499–502.
12. Mirra SS, Heyman A, McKeel D, et al. The Consortium to Establish a Registry for Alzheimer's Disease (CERAD): part II: standardization of the neuropathologic assessment of Alzheimer's disease. Neurology 1991;41:479–486.
13. Braak H, Braak E. Neuropathological stageing of Alzheimer-related changes. Acta Neuropathol 1991;82:239–259.
14. Braak H, Alafuzoff I, Arzberger T, Kretzschmar H, Del Tredici K. Staging of Alzheimer disease-associated neurofibrillary pathology using paraffin sections and immunocytochemistry. Acta Neuropathol 2006;112:389–404.
15. Brown MS, Goldstein JL. A receptor-mediated pathway for cholesterol homeostasis. Science 1986;232:34–47.
16. Saunders AM, Strittmatter WJ, Schmechel D, et al. Association of apolipoprotein E allele epsilon 4 with late-onset familial and sporadic Alzheimer's disease. Neurology 1993;43:1467–1472.
17. Ingelsson E, Schaefer EJ, Contois JH, et al. Clinical utility of different lipid measures for prediction of coronary heart disease in men and women. JAMA 2007;298:776–785.
18. Hardy J. Alzheimer's disease: the amyloid cascade hypothesis: an update and reappraisal. J Alzheimers Dis 2006;9:151–153.
19. Simons M, Keller P, De Strooper B, Beyreuther K, Dotti CG, Simons K. Cholesterol depletion inhibits the generation of beta-amyloid in hippocampal neurons. Proc Natl Acad Sci USA 1998;95:6460–6464.
20. Bodovitz S, Klein WL. Cholesterol modulates alpha-secretase cleavage of amyloid precursor protein. J Biol Chem 1996;271:4436–4440.
21. Hayashi H, Kimura N, Yamaguchi H, et al. A seed for Alzheimer amyloid in the brain. J Neurosci 2004;24:4894–4902.
22. Burns MP, Noble WJ, Olm V, et al. Co-localization of cholesterol, apolipoprotein E and fibrillar Abeta in amyloid plaques. Brain Res Mol Brain Res 2003;110:119–125.
23. Kuo YM, Emmerling MR, Bisgaier CL, et al. Elevated low-density lipoprotein in Alzheimer's disease correlates with brain abeta 1–42 levels. Biochem Biophys Res Commun 1998;252:711–715.
24. Wahrle S, Das P, Nyborg AC, et al. Cholesterol-dependent gamma-secretase activity in buoyant cholesterol-rich membrane microdomains. Neurobiol Dis 2002;9:11–23.
25. Anstey KJ, Lipnicki DM, Low LF. Cholesterol as a risk factor for dementia and cognitive decline: a systematic review of prospective studies with meta-analysis. Am J Geriatr Psychiatry 2008;16:343–354.
26. Notkola IL, Sulkava R, Pekkanen J, et al. Serum total cholesterol, apolipoprotein E epsilon 4 allele, and Alzheimer's disease. Neuroepidemiology 1998;17:14–20.
27. Kivipelto M, Helkala EL, Laakso MP, et al. Apolipoprotein E epsilon4 allele, elevated midlife total cholesterol level, and high midlife systolic blood pressure are independent risk factors for late-life Alzheimer disease. Ann Intern Med 2002;137:149–155.
28. Whitmer RA, Sidney S, Selby J, Johnston SC, Yaffe K. Midlife cardiovascular risk factors and risk of dementia in late life. Neurology 2005;64:277–281.
29. Solomon A, Kivipelto M, Wolozin B, Zhou J, Whitmer RA. Midlife serum cholesterol and increased risk of Alzheimer's and vascular dementia three decades later. Dement Geriatr Cogn Disord 2009;28:75–80.
30. Mielke MM, Zandi PP, Sjogren M, et al. High total cholesterol levels in late life associated with a reduced risk of dementia. Neurology 2005;64:1689–1695.
31. Mielke MM, Zandi PP, Shao H, et al. The 32-year relationship between cholesterol and dementia from midlife to late life. Neurology 2010;75:1888–1895.

Psychiatry and Clinical Neurosciences 2011; **65**: 280–285 doi:10.1111/j.1440-1819.2011.02193.x

Regular Article

Nominal association between a polymorphism in *DGKH* and bipolar disorder detected in a meta-analysis of East Asian case–control samples

Atsushi Takata, MD,[1,3] Hiroaki Kawasaki, MD, PhD,[1]* Yoshimi Iwayama, MS,[2] Kazuo Yamada, MD, PhD,[2] Leo Gotoh, PhD,[1] Hiroshi Mitsuyasu, MD, PhD,[1] Tomofumi Miura, MD, PhD,[1] Tadafumi Kato, MD, PhD,[3] Takeo Yoshikawa, MD, PhD[1] and Shigenobu Kanba, MD, PhD[1]

[1]*Department of Neuropsychiatry, Graduate School of Medical Sciences, Kyushu University, Fukuoka, and Laboratories for* [2]*Molecular Psychiatry and* [3]*Molecular Dynamics of Mental Disorders, RIKEN Brain Science Institute, Saitama, Japan*

Aim: Recent genome-wide association studies (GWAS) of bipolar disorder (BD) have detected new candidate genes, including *DGKH*, *DFNB31* and *SORCS2*. However, the results of these GWAS were not necessarily consistent, indicating the importance of replication studies. In this study, we tested the genetic association of *DGKH*, *DFNB31* and *SORCS2* with BD.

Methods: We genotyped 18 single-nucleotide polymorphisms (SNP) in *DGKH*, *DFNB31* and *SORCS2* using Japanese samples (366 cases and 370 controls). We also performed a meta-analysis of four SNP in *DGKH*, using the previously published allele frequency data of Han-Chinese case–control samples (1139 cases and 1138 controls).

Results: In the association analysis using Japanese samples, a SNP in *SORCS2* (rs10937823) showed nominal genotypic association. However, we could not find any association in an additional analysis of tag SNP around rs10937823. In the meta-analysis of SNP in *DGKH*, rs9315897, which was not significantly associated with BD in the previous Chinese study, showed nominal association.

Conclusion: Although the association was not strong, the result of this study would support the association between *DGKH* and BD.

Key words: DFNB31, genome-wide association studies, manic–depressive illness, mood disorder, SORCS2.

FAMILY, TWIN AND adoption studies have consistently demonstrated the contribution of inherited genetic variation on risk for bipolar disorder (BD).[1] Therefore, numerous genetic studies, including linkage mapping and candidate gene studies, have been carried out. However, the results of these studies have largely been inconsistent. After the era of linkage study and candidate gene approach, genome-wide association studies (GWAS), which investigate 500 000 to 1 000 000 single-nucleotide polymorphisms (SNP) throughout the genome using DNA microarray, have become popular. For BD, an increasing number of GWAS, including meta-analyses, have been conducted.[2–7,16,17] Meta-analyses of GWAS data of BD and major depressive disorder were also performed.[8,9] These studies identified many previously unsuspected candidate genes.

DGKH, *DFNB31* and *SORCS2* are included in these new candidate genes for BD, as well as other promising genes, such as *ANK3*, *CACNA1C*,[3] *PBRM1*[8] and so on. The association of *DGKH*, *DFNB31* and

Correspondence: Hiroaki Kawasaki, MD, PhD, Department of Neuropsychiatry, Graduate School of Medical Sciences, Kyushu University, 3-1-1, Maidashi, Higashi-ku, Fukuoka 812-8582, Japan. Email: hiroakik@npsych.med.kyushu-u.ac.jp
Received 12 August 2010; revised 15 December 2010; accepted 12 January 2011.

SORCS2 with BD was identified in the first reported GWAS using a DNA pooling strategy followed by individual genotyping.[2] All of these genes are expressed in the brain and have some functional implication with neuropsychiatric disorders. Diacylglycerol kinase (DGK) eta, encoded by *DGKH*, is a member of the DGK family that plays an important role in the inositol pathway, the putative site of action of lithium.[10] *DFNB31* encodes whirlin, which is also known as Cip98. This protein interacts with a calmodulin-dependent serine kinase and is suggested to be involved in the formation of scaffolding protein complex and in synaptic transmission.[11] A mutation in this gene is known to cause Usher syndrome,[12] which is characterized by hearing impairment and progressive vision loss. One study reported frequent comorbidity of bipolar disorder or depressive disorder in Usher syndrome patients.[13] *SORCS2*, encoding a VSP10 domain containing-receptor, is expressed in both the developing and adult brain.[14] While the ligand for SORCS2 is so far unknown, highly homologous other members of the SORCS VSP10 domain-containing-receptor family, SORCS1 and SORCS3, are known to bind several growth factors, such as NGF and PDGF.[15] These findings further make *DGKH*, *DFNB31* and *SORCS2* good candidates for BD. However, GWAS usually investigate hundreds of thousands SNP and always involve the potential for false positive results. In fact, some inconsistent results about these genes were reported in other GWAS for BD.[3–7,16,17]

Several replication studies of *DGKH*, *DFNB31* and *SORCS2* were also reported and they include both positive and negative results. A study in Sardinian samples (197 cases and 300 controls) detected a haplotypic association between BD and *DGKH*.[18] Another study that examined 36 tag SNP from *DGKH* in a Scandinavian population (594 cases and 1421 controls) reported no association.[19] A replication study of GWAS that investigated 26 SNP, including those from *DGKH*, *DFNB31* and *SORCS2* using a Finnish family cohort (723 individuals from 180 families), reported associations of *DFNB31* and *SORCS2* but no association of *DGKH* with BD.[20] Recently, Zeng *et al.* reported a strong haplotypic association (minimum $P = 3.87 \times 10^{-6}$) between *DGKH* and BD in a Han-Chinese case–control cohort.[21]

In this study, we investigated associations of *DGKH*, *DFNB31* and *SORCS2* with BD using Japanese case–control samples (366 cases and 370 controls). Furthermore, we conducted a meta-analysis of four SNP in *DGKH*, which are overlapped with the SNP investigated by Zeng *et al.* In total, 1505 cases and 1508 control samples were used for the meta-analysis.

METHODS

The Japanese case–control samples consisted of 366 patients with bipolar I disorder (BDI), bipolar II disorder (BDII) or schizoaffective disorder bipolar type (SAB) (257 BDI, 104 BDII and five SAB; 181 men and 185 women, aged 50.1 ± 13.4 years) and 370 control subjects (185 men and 185 women aged 50.6 ± 12.6 years). All subjects were unrelated and ethnically Japanese. The patients were diagnosed by at least two experienced psychiatrists according to the DSM-IV criteria on the basis of unstructured interviews and reviews of their medical records. All healthy control subjects were also psychiatrically screened on the basis of unstructured interviews. The objective of the present study was clearly explained, and written informed consent was obtained from all the participants. The characteristics of the Han-Chinese cohort used for meta-analysis were described elsewhere.[21] This study was approved by the ethics committees of Kyushu University Graduate School of Medicine and RIKEN Brain Science Institute.

For SNP selection, we focused on the SNP that were reported in a previous GWAS by Baum *et al.* and that cause non-synonymous amino acid substitutions and possibly affect the function of encoded proteins. SNP chosen from Baum *et al.* included six SNP whose associations were detected in the follow-up individual genotyping (three in *DGKH*, one in *DFNB31* and two in *SORCS2*, reported *P*-values ranging from 0.0005 to 1.5×10^{-8}). Three SNP in *DGKH* indicated to be associated in both of the two independent pooling sample sets were additionally selected. The selected non-synonymous SNP consisted of two SNP in *DGKH*, five SNP in *DFNB31* and two SNP in *SORCS2*. The total number of selected SNP was eighteen. Genotyping was performed using TaqMan assay (Applied Biosystems, Foster City, CA, USA). Differences in allele and genotype frequencies between BD and controls were evaluated with Fisher's exact test. Deviations from Hardy–Weinberg equilibrium (HWE), structures of linkage disequilibrium (LD) blocks and haplotypic associations were analyzed using Haploview version 4.1 software,[22] (http://www.broadinstitute.org/scientific-community/science/programs/medical-and-population-genetics/

haploview/haploview). A meta-analysis using the Mantel–Haenszel model and evaluation of sample heterogeneity were performed on Review Manager.[23] The I^2 statistics[24,25] were used for the assessment of heterogeneity between the samples.

RESULTS

The results of genotyping in the Japanese cohort are summarized in Table 1. Three SNP (rs35776153, rs35003670 and rs34058821) registered in dbSNP (http://www.ncbi.nlm.nih.gov/projects/SNP/) were not polymorphic in our samples. Genotype frequencies of each SNP were in HWE ($P > 0.05$) except for rs16840892 in the BD group. No SNP displayed significant allelic association with BD. A nominally significant genotypic association was observed with rs10937823 of *SORCS2*. However, the over-represented allele in BD was opposite to the one that was reported in a previous GWAS (T in this study and C in Baum *et al.*). To investigate this locus more intensively, we selected four tag SNP in the region between rs4411993 and rs34058821 (physical chromosomal position spanning 7 517 366 to 7 717 060), using TAG SNP Selection,[26] http://manticore.niehs.nih.gov/), and genotyped them. However, no significant allelic or genotypic association between these four SNP and BD was found (Table 1, with ‡).

In LD structure analysis, two LD blocks in *DGKH* and one block in each of *DFNB31* and *SORCS2* were detected. In haplotype analysis, a total of 14 haplotypes whose frequencies were more than 1% were estimated, but no significant haplotypic associations with BD were detected (data not shown).

The results of the meta-analysis are shown in Table 2. We found a nominal association in rs9315897 ($P = 0.039$), which was not significantly associated with BD in Zeng *et al.* No sample heterogeneity was observed in the four investigated SNP.

DISCUSSION

In this study, we performed association analyses of *DGKH*, *DFNB31* and *SORCS2* with BD in Japanese case–control samples. We also conducted a meta-analysis of four SNP in *DGKH* using the data from the present Japanese cohort and previously reported Han-Chinese cohort.

The results of association analyses in the Japanese cohort were largely inconsistent with the initial study.[2] Among GWAS, while partly common associations of *DFNB31* (in Sklar *et al.*[4] and WTCCC[6], minimum *P*-value was 8.8×10^{-6}) and *SORCS2* (in Smith *et al.*,[5] minimum *P*-value was 0.009) were found, largely inconsistent results for these genes were also reported. From the results of GWAS for BD and other complex traits, the effect of a single common variant has been recognized to be relatively low (odds ratio [OR] less than 1.5, often 1.1–1.2[27]), with some exceptional genes containing common high-risk markers, such as *APOE* for Alzheimer's disease and *CFH* and *ARMS2/HTRA1* for age-related macular degeneration. In this study, statistical powers of the Japanese cohort calculated with allele frequencies of our Japanese control samples and OR 1.3 for an alpha level of 0.05 or 0.002 (0.05 divided by the numbers of tested SNP) were 71.7 or 28.9% for *DGKH*, 61.3 or 19.9% for *DFNB31*, and 56.8 or 16.9% for *SORCS2* (calculated with the Genetic Power Calculator,[28] http://statgen.iop.kcl.ac.uk/gpc/). Therefore, the sample number was not sufficient to detect risk-conferring markers with small effects. As a reason for inconsistent results, the adverse effect of population stratification should also be considered. In this study, all participants were recruited in the central area of Japan. Previous studies reported no substantial stratification in this population.[17,29] In particular, samples in Hattori *et al.*[17] were part of the samples used for this study, indicating that false positive results due to the effect of population stratification could be avoided.

In the meta-analysis, we found a nominal but significant association between rs9315897 in *DGKH* and BD. The total number of samples used for meta-analysis was larger than 3000. Thus, this result was more reliable than the result solely from the Japanese cohort. Although the association was not strong as was reported in Baum *et al.*, and did not overcome a correction for multiple testing, this result may indicate this SNP as a risk marker common across ethnicities.

In conclusion, we found a nominal association between a polymorphism in *DGKH* and BD in the meta-analysis using more than 3000 samples from East Asia. However, the association was not strong and further investigations are required to obtain a conclusive result. For polymorphisms in *SORCS2* and *DFNB31*, the statistical power obtained solely from our Japanese samples was apparently insufficient to detect risk markers with weak effect. However, this data also have a particular meaning, because they could be utilized in future meta-analysis.

Table 1. Allele and genotype frequencies of SNP in *DGKH, DFNB31* and *SORCS2* in the case–control sample

Gene	SNP ID		HWE *P*-value	*n*	Allele		*P*-value (Fisher's exact test)	Genotype			*P*-value (Fisher's exact test)	MAF
DGKH					T	C		T/T	T/C	C/C		
	rs9315885	BD	0.5045	364	333	395		73	187	104		45.7%
		CT	0.9530	370	336	404	0.9166	76	184	110	0.9094	45.4%
					A	C		A/A	A/C	C/C		
	rs1012053	BD	0.4608	364	359	369		85	189	90		49.3%
		CT	0.9595	369	366	372	0.9169	91	184	94	0.8578	49.6%
					A	G		A/A	A/G	G/G		
	rs1170195	BD	0.2023	360	352	368		80	192	88		51.1%
		CT	0.7547	370	372	368	0.6011	92	188	90	0.6789	49.7%
					T	C		T/T	T/C	C/C		
	rs9525570	BD	0.7813	360	615	105		262	91	7		14.6%
		CT	0.7634	368	645	91	0.2201	282	81	5	0.4520	12.4%
					C	T		C/C	C/T	T/T		
	rs1170191	BD	0.2748	358	373	343		92	189	77		47.9%
		CT	0.9982	368	364	372	0.3190	90	184	94	0.4430	50.5%
					T	C		T/T	T/C	C/C		
	rs9315897	BD	0.8558	364	623	105		267	89	8		14.4%
		CT	0.6845	369	645	93	0.3211	281	83	5	0.5399	12.6%
					C	T		C/C	C/T	T/T		
	rs35776153†	BD	N/A	365	730	0		365	0	0		0.0%
		CT	N/A	370	740	0	1.0000	370	0	0	1.0000	0.0%
					T	C		T/T	T/C	C/C		
	rs17646069†	BD	0.5476	365	634	96		274	86	5		13.2%
		CT	0.0858	370	632	108	0.4508	274	84	12	0.2630	14.6%
DFNB31					T	G		T/T	T/G	G/G		
	rs2274158†	BD	0.8790	362	283	441		56	171	135		39.1%
		CT	0.5230	369	305	433	0.3937	66	173	130	0.6525	41.3%
					A	G		A/A	A/G	G/G		
	rs2274159†	BD	0.4654	364	336	392		81	174	109		46.2%
		CT	0.9039	369	347	391	0.7536	81	185	103	0.7906	47.0%
					A	G		A/A	A/G	G/G		
	rs942519†	BD	0.5699	364	320	408		73	174	117		44.0%
		CT	0.8110	370	329	411	0.8747	72	185	113	0.8363	44.5%
					T	C		T/T	T/C	C/C		
	rs4978584†	BD	0.9308	365	290	440		58	174	133		39.7%
		CT	0.4675	370	302	438	0.7097	65	172	133	0.8363	40.8%
					C	G		C/C	C/G	G/G		
	rs35003670†	BD	N/A	362	724	0		362	0	0		0.0%
		CT	N/A	370	740	0	1.0000	370	0	0	1.0000	0.0%
					A	G		A/A	A/G	G/G		
	rs942518	BP	0.2645	363	563	163		222	119	22		22.5%
		CT	0.4526	370	561	179	0.4587	210	141	19	0.3087	24.2%
SORCS2					T	C		T/T	T/C	C/C		
	rs4411993	BD	0.8482	360	227	493		35	157	168		31.5%
		CT	0.2895	367	221	513	0.5703	29	163	175	0.6969	30.1%
					G	C		G/G	G/C	C/C		
	rs11736984‡	BP	0.2064	364	192	536		30	132	202		26.4%
		CT	0.1696	369	184	554	0.5499	18	148	203	0.1457	24.9%

Table 1. (*Continued*)

Gene	SNP ID		HWE *P*-value	*n*	Allele		*P*-value (Fisher's exact test)	Genotype			*P*-value (Fisher's exact test)	MAF
					T	C		T/T	T/C	C/C		
	rs10937823	BD	0.0500	363	200	526		35	130	198		27.5%
		CT	0.0681	370	187	553	0.3432	17	153	200	0.0175*	25.3%
					G	C		G/G	G/C	C/C		
	rs13139074‡	BP	0.4360	366	206	526		32	142	192		28.1%
		CT	0.3993	367	188	546	0.2891	21	146	200	0.2929	25.6%
					A	G		A/A	A/G	G/G		
	rs11734984‡	BP	0.4737	363	206	520		32	142	189		28.4%
		CT	0.8256	370	203	537	0.7268	27	149	194	0.7501	27.4%
					T	C		T/T	T/C	C/C		
	rs12645507‡	BP	0.0801	365	449	281		146	157	62		38.5%
		CT	0.9372	368	472	264	0.3049	151	170	47	0.2682	35.9%
					G	A		G/G	G/A	A/A		
	rs34058821†	BD	N/A	366	732	0		366	0	0		0.0%
		CT	N/A	369	738	0	1.0000	369	0	0	1.0000	0.0%
					T	C		T/T	T/C	C/C		
	rs16840892†	BD	0.0254	364	254	474		54	146	164		34.9%
		CT	0.2437	370	255	485	0.8695	49	157	164	0.7480	34.5%

*$P < 0.05$.
†Non-synonymous SNP.
‡Additionally examined SNP.
BD, bipolar disorder sample; CT, control sample; HWE, Hardy–Weinberg equilibrium; MAF, minor allele frequency; *n*, number of genotyped participants; SNP, single-nucleotide polymorphism.

Table 2. Result of the meta-analysis of four SNP in *DGKH*

	Present study				Zeng *et al.*[21]				Meta-analysis	
	MAF†				MAF†					
SNP, minor allele†	Cases ($n = 366$)	Controls ($n = 370$)	*P*	OR (95%CI)	Cases ($n = 1139$)	Controls ($n = 1138$)	*P*	OR (95%CI)	*P*	OR (95%CI)
rs9315885, T	0.457	0.454	0.9166	1.01 (0.83,1.24)	0.493	0.482	0.453	1.04 (0.93,1.17)	0.478‡	1.04 (0.94,1.15)
rs1012053, A	0.493	0.496	0.9169	0.99 (0.81,1.21)	0.527	0.507	0.191	1.08 (0.97,1.22)	0.258‡	1.06 (0.96,1.17)
rs1170191, C	0.521	0.495	0.3190	1.11 (0.90,1.37)	0.528	0.508	0.179	1.08 (0.97,1.22)	0.093‡	1.09 (0.99,1.21)
rs9315897, C	0.144	0.126	0.3211	1.17 (0.87,1.58)	0.111	0.095	0.089	1.19 (0.98,1.44)	0.039*‡	1.18 (1.01,1.39)

*$P < 0.05$.
†Minor alleles in the Japanese control samples.
‡Test for heterogeneity: $I^2 = 0\%$.
CI, confidence interval; MAF, minor allele frequency; OR, odds ratio; SNP, single-nucleotide polymorphism.

ACKNOWLEDGMENTS

This study was supported in part by Health and Labour Sciences Research Grants (Research on Psychiatric and Neurological Diseases and Mental Health [2006–012] Neurophysiology, neuroimaging, and molecular biology of bipolar disorders).

REFERENCES

1. Taylor L, Faraone SV, Tsuang MT. Family, twin, and adoption studies of bipolar disease. *Curr. Psychiatry Rep.* 2002; **4**: 130–133.
2. Baum AE, Akula N, Cabanero M *et al.* A genome-wide association study implicates diacylglycerol kinase eta (DGKH) and several other genes in the etiology of bipolar disorder. *Mol. Psychiatry* 2008; **13**: 197–207.
3. Ferreira MA, O'Donovan MC, Meng YA *et al.* Collaborative genome-wide association analysis supports a role for ANK3 and CACNA1C in bipolar disorder. *Nat. Genet.* 2008; **40**: 1056–1058.
4. Sklar P, Smoller JW, Fan J *et al.* Whole-genome association study of bipolar disorder. *Mol. Psychiatry* 2008; **13**: 558–569.
5. Smith EN, Bloss CS, Badner JA *et al.* Genome-wide association study of bipolar disorder in European American and African American individuals. *Mol. Psychiatry* 2009; **14**: 755–763.
6. WTCCC. Genome-wide association study of 14,000 cases of seven common diseases and 3,000 shared controls. *Nature* 2007; **447**: 661–678.
7. Lee MT, Chen CH, Lee CS *et al.* Genome-wide association study of bipolar I disorder in the Han Chinese population. *Mol. Psychiatry* 2010 (in press).
8. McMahon FJ, Akula N, Schulze TG *et al.* Meta-analysis of genome-wide association data identifies a risk locus for major mood disorders on 3p21.1. *Nat. Genet.* 2010; **42**: 128–131.
9. Liu Y, Blackwood DH, Caesar S *et al.* Meta-analysis of genome-wide association data of bipolar disorder and major depressive disorder. *Mol. Psychiatry* 2011; **16**: 2–4.
10. Berridge MJ. The Albert Lasker Medical Awards. Inositol trisphosphate, calcium, lithium, and cell signaling. *JAMA* 1989; **262**: 1834–1841.
11. Yap CC, Liang F, Yamazaki Y *et al.* CIP98, a novel PDZ domain protein, is expressed in the central nervous system and interacts with calmodulin-dependent serine kinase. *J. Neurochem.* 2003; **85**: 123–134.
12. Mburu P, Mustapha M, Varela A *et al.* Defects in whirlin, a PDZ domain molecule involved in stereocilia elongation, cause deafness in the whirler mouse and families with DFNB31. *Nat. Genet.* 2003; **34**: 421–428.
13. Tamayo ML, Maldonado C, Plaza SL *et al.* Neuroradiology and clinical aspects of Usher syndrome. *Clin. Genet.* 1996; **50**: 126–132.
14. Hermey G, Plath N, Hubner CA, Kuhl D, Schaller HC, Hermans-Borgmeyer I. The three sorCS genes are differentially expressed and regulated by synaptic activity. *J. Neurochem.* 2004; **88**: 1470–1476.
15. Hermey G. The Vps10p-domain receptor family. *Cell. Mol. Life Sci.* 2009; **66**: 2677–2689.
16. Scott LJ, Muglia P, Kong XQ *et al.* Genome-wide association and meta-analysis of bipolar disorder in individuals of European ancestry. *Proc. Natl. Acad. Sci. USA* 2009; **106**: 7501–7506.
17. Hattori E, Toyota T, Ishitsuka Y *et al.* Preliminary genome-wide association study of bipolar disorder in the Japanese population. *Am. J. Med. Genet. B Neuropsychiatr. Genet.* 2009; **150B**: 1110–1117.
18. Squassina A, Manchia M, Congiu D *et al.* The diacylglycerol kinase eta gene and bipolar disorder: a replication study in a Sardinian sample. *Mol. Psychiatry* 2009; **14**: 350–351.
19. Tesli M, Kahler AK, Andreassen BK *et al.* No association between DGKH and bipolar disorder in a Scandinavian case-control sample. *Psychiatr. Genet.* 2009; **19**: 269–272.
20. Ollila HM, Soronen P, Silander K *et al.* Findings from bipolar disorder genome-wide association studies replicate in a Finnish bipolar family-cohort. *Mol. Psychiatry* 2009; **14**: 351–353.
21. Zeng Z, Wang T, Li T *et al.* Common SNPs and haplotypes in DGKH are associated with bipolar disorder and schizophrenia in the Chinese Han population. *Mol. Psychiatry* 2010 (in press).
22. Barrett JC, Fry B, Maller J, Daly MJ. Haploview: analysis and visualization of LD and haplotype maps. *Bioinformatics* 2005; **21**: 263–265.
23. *Review Manager (RevMan)* [Computer program]. Version 5.0. The Nordic Cochrane Centre, The Cochrane Collaboration, Copenhagen, 2008.
24. Higgins JP, Thompson SG. Controlling the risk of spurious findings from meta-regression. *Stat. Med.* 2004; **23**: 1663–1682.
25. Trikalinos TA, Salanti G, Zintzaras E, Ioannidis JP. Meta-analysis methods. *Adv. Genet.* 2008; **60**: 311–334.
26. Xu Z, Taylor JA. SNPinfo: integrating GWAS and candidate gene information into functional SNP selection for genetic association studies. *Nucleic Acids Res.* 2009; **37**: W600–W605.
27. Spencer CC, Su Z, Donnelly P, Marchini J. Designing genome-wide association studies: sample size, power, imputation, and the choice of genotyping chip. *PLoS Genet.* 2009; **5**: e1000477.
28. Purcell S, Cherny SS, Sham PC. Genetic Power Calculator: design of linkage and association genetic mapping studies of complex traits. *Bioinformatics* 2003; **19**: 149–150.
29. Yamaguchi-Kabata Y, Nakazono K, Takahashi A *et al.* Japanese population structure, based on SNP genotypes from 7003 individuals compared to other ethnic groups: effects on population-based association studies. *Am. J. Hum. Genet.* 2008; **83**: 445–456.

Schizophrenia Research 129 (2011) 172–182

Contents lists available at ScienceDirect

Schizophrenia Research

journal homepage: www.elsevier.com/locate/schres

Aripiprazole inhibits superoxide generation from phorbol-myristate-acetate (PMA)-stimulated microglia in vitro: Implication for antioxidative psychotropic actions via microglia

Takahiro A. Kato [a,b,*], Akira Monji [a,*], Keiji Yasukawa [b,c], Yoshito Mizoguchi [a], Hideki Horikawa [a], Yoshihiro Seki [a], Sadayuki Hashioka [a], Youn-Hee Han [c,d], Mina Kasai [a], Noriyuki Sonoda [b,e], Eiichi Hirata [b,e], Yasutaka Maeda [b,e], Toyoshi Inoguchi [b,e], Hideo Utsumi [b], Shigenobu Kanba [a]

[a] Department of Neuropsychiatry, Graduate School of Medical Sciences, Kyushu University, Maidashi 3-1-1, Higashi-ku, Fukuoka 812-8582, Japan
[b] Innovation Center for Medical Redox Navigation, Kyushu University, Maidashi 3-1-1, Higashi-ku, Fukuoka 812-8582, Japan
[c] Department of Chemo-Pharmaceutical Sciences, Graduate School of Pharmaceutical Sciences, Kyushu University, 3-1-1 Maidashi Higashi-ku, Fukuoka 812-8582, Japan
[d] Department of Civil and Environmental Engineering, Tohoku Gakuin University, 1-13-1 Chou, Tagajo, 985-8537, Japan
[e] Department of Internal Medicine and Bioregulatory Science, Graduate School of Medical Sciences, Kyushu University, Maidashi 3-1-1, Higashi-ku, Fukuoka 812-8582, Japan

ARTICLE INFO

Article history:
Received 1 October 2010
Received in revised form 20 March 2011
Accepted 21 March 2011
Available online 15 April 2011

Keywords:
Microglia
Schizophrenia
Oxidative stress
Antipsychotics
Superoxide
NADPH oxidase

ABSTRACT

Altered antioxidant status has been implicated in schizophrenia. Microglia, major sources of free radicals such as superoxide ($\bullet O_2^-$), play crucial roles in various brain pathologies. Recent postmortem and imaging studies have indicated microglial activation in the brain of schizophrenic patients. We previously demonstrated that atypical antipsychotics including aripiprazole significantly inhibited the release of nitric oxide and proinflammatory cytokines from interferon-γ-stimulated microglia in vitro. Antioxidative effects of antipsychotics via modulating microglial superoxide generation have never been reported. Therefore, we herein investigated the effects of antipsychotics on the $\bullet O_2^-$ generation from phorbol-myristate-acetate (PMA)-stimulated rodent microglia by the electron spin resonance (ESR) spectroscopy and also examined the intracellular mechanism by intracellular Ca^{2+} imaging and immunostaining. Neuronal damage induced by microglial activation was also investigated by the co-culture experiment.

Among various antipsychotics, only aripiprazole inhibited the $\bullet O_2^-$ generation from PMA-stimulated microglia. Aripiprazole proved to inhibit the $\bullet O_2^-$ generation through the cascade of protein kinase C (PKC) activation, intracellular Ca^{2+} regulation and NADPH oxidase activation via cytosolic $p47^{phox}$ translocation to the plasma/phagosomal membranes. Formation of neuritic beading, induced by PMA-stimulated microglia, was attenuated by pretreatment of aripiprazole.

D2R antagonism has long been considered as the primary therapeutic action for schizophrenia. Aripiprazole with D2R partial agonism is effective like other antipsychotics with fewer side effects, while aripiprazole's therapeutic mechanism itself remains unclear. Our results imply that aripiprazole may have psychotropic effects by reducing the microglial oxidative reactions and following neuronal reactions, which puts forward a novel therapeutic hypothesis in schizophrenia research.

1. Introduction

Altered antioxidant status has recently been implicated in schizophrenia with increasing number of clinical evidence measuring biochemical components for detoxification of reactive oxygen species (ROS) such as glutathione (GSH) and superoxide dismutase (SOD) (Do et al., 2009; Ng et al., 2008; Yao et al., 2001; Zhang et al., 2009a). A recent postmortem study and a cerebral spectroscopic study indicated a positive relationship between oxidative stress and schizophrenia (Treasaden and Puri, 2008; Wang et al., 2009). Overproduction of neutrophil ROS has reported to correlate with negative symptoms in schizophrenia (Sirota et al., 2003). Ketamine, which can lead to a syndrome indistinguishable from schizophrenia, has recently been

Abbreviations: DMSO, dimethyl sulfoxide; DPI, diphenylene iodonium; D2R, dopamine D2 receptor; ESR, electron spin resonance; GSH, glutathione; GM-CSF, granulocyte macrophage colony stimulating factor; $[Ca^{2+}]i$, intracellular Ca^{2+} concentration; NAC, N-Acetyl cysteine; NGF, nerve growth factor; NO, nitric oxide; PKC, protein kinase C; ROS, reactive oxygen species; $\bullet O_2^-$, superoxide; SOD, superoxide dismutase; TNF-α, tumor necrosis factor-α.

* Corresponding authors at: Department of Neuropsychiatry, Graduate School of Medical Sciences, Kyushu University, Maidashi 3-1-1, Higashi-ku, Fukuoka 812-8582, Japan. Tel.: +81 92 642 5627; fax: +81 92 642 5644.
E-mail addresses: takahiro@npsych.med.kyushu-u.ac.jp (T.A. Kato), amonji@hf.rim.or.jp (A. Monji).

0920-9964/$ – see front matter © 2011 Elsevier B.V. All rights reserved.
doi:10.1016/j.schres.2011.03.019

reported to induce a persistent increase in brain superoxide radicals due to activation of NADPH oxidase (Behrens et al., 2007). On the other hand, N-Acetyl cysteine (NAC), a glutathione precursor, has recently been reported to be effective for augmentation therapy of chronic schizophrenia and to improve impaired mismatch negativity in schizophrenic patients (Berk et al., 2008; Lavoie et al., 2008). More recently, the serum levels of SOD in chronic patients with schizophrenia are associated with psychopathology and response to antipsychotics (Zhang et al., 2009b). These findings suggest that regulation of oxidative stress may be related to the pathophysiology and therapeutic mechanism of schizophrenia.

Microglia, major sources of free radicals such as superoxide ($\bullet O_2^-$) and nitric oxide (NO) in the CNS, play a crucial role in variety of brain pathologies (Block and Hong, 2005; Block et al., 2007; Hanisch and Kettenmann, 2007). The pathophysiology of schizophrenia remains unclear, while recent postmortem brain studies using class II human leucocyte antigen (HLA-DR) have revealed microglial activation in the brains of schizophrenic patients (Radewicz et al., 2000; Steiner et al., 2008). Positron emission computed tomography (PET) studies with specific ligand of the peripheral benzodiazepine-binding sites (PBBS), have indicated that activated microglia may be present in schizophrenic patients (Doorduin et al., 2009; Takano et al., 2010; van Berckel et al., 2008). There is accumulated evidence that gene–environmental interaction via various factors such as virus infections and social stress leads to development of schizophrenia (Dalman et al., 2008; Jia et al., 2010; Mortensen et al., 2010; van Winkel et al., 2008). Microglia is one of the key players in brain damages induced by virus infections in the CNS (Block et al., 2007). One recent experiment suggested that social stress – isolation – induces NADPH oxidase activation via microglia in rat brain (Schiavone et al., 2009). These reports indicate that microglia may play an important role in gene–environmental interaction associated with schizophrenia (Sawa et al., 2004; Seshadri et al., 2010).

Dopamine system dysfunction has been for long time hypothesized in the pathology of schizophrenia, and dopamine D2 receptor (D2R) antagonism against dopamine neurons has been considered as the primary therapeutic target for schizophrenia (Kapur and Mamo, 2003; Miyamoto et al., 2005). On the other hand, aripiprazole is a novel unique atypical antipsychotic drug, which is a high-affinity D2R partial agonist (Burris et al., 2002; Shapiro et al., 2003). In spite of its different pharmacological profile, aripiprazole is effective against the positive and negative symptoms of patients with schizophrenia like other antipsychotics with fewer side effects (Leucht et al., 2009; Potkin et al., 2003).

We recently demonstrated that not only atypical antipsychotics with D2R antagonism but also aripiprazole with D2R partial agonism significantly inhibited the release of NO and proinflammatory cytokines such as tumor necrosis factor (TNF)-α on interferon-γ-stimulated microglia in vitro (Bian et al., 2008; Kato et al., 2008; Kato et al., 2007). Therapeutic benefits on psychotic symptoms have been demonstrated by COX-2 inhibitor and minocycline, both of which have proved to inhibit microglial activation (Akhondzadeh et al., 2007; Miyaoka et al., 2008; Muller et al., 2010). Summing up the above-mentioned evidence, we hypothesis that microglia may play a key role in the pathophysiology of schizophrenia by producing free radicals and cytokines in the CNS, and that microglial regulation may be a novel therapeutic target for schizophrenia (Monji et al., 2009).

To the best of our knowledge, antioxidative effects of antipsychotics via modulating microglial superoxide generation have never been reported. Phorbol-myristate-acetate (PMA), a typical activator of protein kinase C (PKC), induces $\bullet O_2^-$ from microglia with the elevation of intracellular calcium (Colton et al., 1992; Sankarapandi et al., 1998; Yoo et al., 1996). PKC has recently been indicated to be associated with stress-related illness and psychiatric disorders (Chen et al., 2009; Hains et al., 2009). Therefore, in the present study, we investigated the effects of various antipsychotics on the generation of $\bullet O_2^-$ from PMA-stimulated microglia by the electron spin resonance (ESR) spectroscopy and also examined the intracellular mechanism by intracellular Ca^{2+} imaging and immunostaining. Neuronal damage induced by microglial activation was also investigated by co-culture experiment.

2. Materials and methods

2.1. Chemicals and reagents

PMA was purchased from Biomol International (Plymouth Meeting, PA, USA). LPS, haloperidol, clozapine, a D2R full agonist; quinpirole, NADPH oxidase inhibitors; diphenylene iodonium (DPI) and apocynin, and a spin trap; DEPMPO were purchased from Sigma Chemicals (St. Louis, MO, USA). SOD, catalase, xanthine, and xanthine oxidase were purchased from Wako Pure Chemical Industries (Osaka, Japan). Recombinant mouse GM-CSF was purchased from R&D systems (Minneapolis, MN, USA). WST-8 was purchased from Dojindo Molecular Technologies (Kumamoto, Japan). Atypical antipsychotics were generously provided by each manufacturer; aripiprazole from Otsuka Pharmaceutical Co., Ltd. (Tokyo, Japan), risperidone from Janssen Pharmaceutica NV (Beerse, Belgium), and olanzapine from Eli Lilly and Co. (Indianapolis, IN, USA). Antipsychotics were dissolved initially into 20 mM with dimethyl sulfoxide (DMSO) and then were diluted into final concentration for each experiment. The final concentrations of antipsychotics were not over 10 μM. All antipsychotics and DMSO at the highest concentration (0.05%) were confirmed not to be toxic to microglial cells in our previous reports (Kato et al., 2007, 2008).

2.2. Cell cultures

All experimental procedures were conducted in accordance with the Standard Guidelines for Animal Experiments of Kyushu University. Rat primary microglial cells were cultured as previously described (Kato et al., 2008; Seki et al., 2010). Briefly, primary mixed cells were prepared from the whole brain of the 3-day-postnatal Sprague–Dawley rats, using Cell Strainer (BD Falcon, Franklin Lakes, NJ). Primary rat microglial cells were selected after attachment to Aclar film (Nisshin EM, Tokyo, Japan) for 2 h in Dulbecco's Modified Eagle's Medium supplemented with 10% fetal bovine serum (10% FBS/DMEM). Aclar films were slightly washed by PBS and then transferred to fresh 10% FBS/DMEM, and the fresh microglia was expanded for 1–2 days. The purity of the isolated microglia was assessed by immunocytochemical staining for microglial marker, Iba-1, and >99% of cells were stained positively. Murine microglial 6-3 cells, which was established from neonatal C57BL/6J(H-2b) mice using a non-enzymatic and non-virus-transformed procedure and which closely resemble primary cultured microglia (Kanzawa et al., 2000; Sawada et al., 1998), were cultured as previously described (Bian et al., 2008; Kato et al., 2007). The rat pheochromocytoma PC12 cells were cultured as previously described (Bian et al., 2008). Briefly, the 6-3 cells and PC12 cells were cultured in Eagle's minimal essential medium, 0.3% $NaHCO_3$, 2 mM glutamine, 0.2% glucose, 10 g/mL insulin and 10% fetal calf serum, and then were maintained at 37 °C in a 5% CO_2 and 95% air atmosphere.

2.3. Measurements of superoxide production

2.3.1. Electron spin resonance (ESR) spectroscopy

ESR, together with the spin-trapping agent DEPMPO was employed to accurately detect the production of $\bullet O_2^-$ from PMA-stimulated microglia. We previously described the detail methodology of the ESR (Hashioka et al., 2007a, 2007b). Briefly, the 6-3 cells were cultured on 12-well tissue plates at the density of 1.6×10^6 cells in 400 mL of serum-free medium per well. The 6-3 cells were incubated with 400 ng/mL PMA for 30 min in both the presence and absence of pretreatment of the antipsychotics for 5 h at 37 °C before beginning the detection of ESR spectra. Cell suspensions (4×10^6 cells/

mL) in the culture medium containing 25 mM DEPMPO were transferred to a standard cell capillary, and the ESR measurements were performed at room temperature right after the incubation. The ESR spectra were obtained using a JES-RE1X ESR spectrometer (JEOL, Japan). The setting conditions of the instrument were as follows: magnetic field = 336.7 + 7.5 mT, modulation amplitude = 2000, modulation width = 0.1 mT, modulation frequency = 100 kHz, time constant = 0.1 s, microwave power = 10 mW, microwave frequency = 9430 MHz, and sweep time = 2 min.

ESR was also applied to the rat primary microglial cells. The cells were cultured on 12-well tissue plates at a much lower density of 1.6×10^4 cells in 400 mL of serum-free culture medium per well due to the difficulty in collecting these cells.

2.3.2. Nitro blue tetrazolium (NBT) assay

The quantification of $\bullet O_2^-$ production in microglial cells was performed with modification of Nitro blue tetrazolium (NBT) assay as previously reported (Choi et al., 2006; Tan and Berridge, 2000). As a water-soluble formazan dye, we used the WST-8 (2-(2-methoxy-4-nitrophenyl)-3-(4-nitrophenyl)-5-(2,4-disulfophenyl)-2H-tetrazolium monosodium salt; Dojindo, Kumamoto, Japan). Briefly, microglial cells grown on 96-well culture plates (5×10^3 cells per well) were pre-incubated in the presence and absence of aripiprazole for 5 h and then the medium was changed to 50 μL chelated medium both in the presence and absence of 50 U/mL SOD at 37 °C. After 30 min of incubation with PMA (400 ng/mL), the supernatants were mixed with 5 μL WST-8 solution. The absorbance was read at 450 nm using a plate reader (Labsystems Multiscan MS). The comparative volumes of $\bullet O_2^-$ production were determined by the difference between the absorbance with SOD and that without SOD.

2.4. Spin trapping in xanthine/xanthine oxidase system

Xanthine oxidase (0.1 U/mL) was incubated with 0.4 mM xanthine in phosphate-buffer (PB) containing 2 mM DTPA and 20 mM DEPMPO in the presence and absence of aripiprazole. Xanthine oxidase was added last to the mixture to start the reaction. The ESR spectra were recorded at room temperature on a JES-RE1X ESR spectrometer. The setting conditions of the instrument were as follows: magnetic field = 336.7 + 7.5 mT, modulation amplitude = 500, modulation width = 0.1 mT, modulation frequency = 100 kHz, time constant = 0.03 s, microwave power = 10 mW, microwave frequency = 9430 MHz and sweep time = 2 min.

2.5. Intracellular Ca^{2+} imaging

The experiments were performed in the external standard solution (in mM: 150 NaCl, 5 KCl, 2 $CaCl_2$, 1 $MgCl_2$, 10 glucose and 10 HEPES, pH 7.4 with Tris-OH) at room temperature as we reported previously (Kato et al., 2008; Mizoguchi et al., 2003, 2009). Intracellular Ca^{2+} concentration ($[Ca^{2+}]i$) in response to PMA application was monitored using fura-2 AM (acetoxymethyl ester) (Grynkiewicz et al., 1985) in rat primary microglial cells. The cells plated on glass-base dish were loaded with 5 μM fura-2 AM (Dojindo, Kumamoto, Japan) for 20 min and washed three times with HEPES buffer before the measurement. During the measurement, while using an inverted microscope (20×; Olympus IX70-22FL, Olympus Co. Tokyo, Japan), external HEPES buffer was constantly perfused (10 mL/min). For fura-2 excitation, the cells were illuminated with two alternating wavelengths, 340 and 380 nm using a computerized system. The emitted light was collected at 510 nm using a cooled CCD camera (C4742-95ER, Hamamatsu Photonics, Hamamatsu, Japan) and images were stored every 5 s. These series of sequential data were analyzed using the AquaCosmos software package (Hamamatsu photonics, Hamamatsu, Japan). The $[Ca^{2+}]i$ was calculated from the ratio (R) of fluorescence recorded at 340 and 380 nm excitation wavelengths for each pixel within a cell boundary (AquaCosmos software). Calibrations (conversion of R340/380 values into calcium concentrations) were performed as described previously (Grynkiewicz et al., 1985). Basal $[Ca^{2+}]i$ was determined from the initial 10 images of each cell recording. A $[Ca^{2+}]i$ signal was defined as an increase in R 340/380 with clear time correlation to the application of PMA.

Increase of $[Ca^{2+}]i$ in response to PMA application was calculated as difference between basal $[Ca^{2+}]i$ and highest $[Ca^{2+}]i$ during the treatment of PMA. All data presented were obtained from at least five dishes and three different cell preparations.

2.6. Morphology and immunofluorescence

NADPH oxidase activation via cytosolic $p47^{phox}$ protein translocation was investigated as previously described (Qian et al., 2008). The 6-3 cells were seeded in non-coated 6-well plates at 5×10^3 cells/well. They were incubated in both the absence and presence of aripiprazole, diphenylene iodonium (DPI) or apocynin for 5 h respectively, and then treated with 400 ng/mL PMA for 30 min. After being rinsed twice in 0.1 M Hepes/KOH, cells were fixed with 4% paraformaldehyde for 10 min, and then rinsed with 0.1 M Hepes/KOH for 10 min. The morphological changes of the cells were examined under phase contrast microscopy (Nikon, Tokyo, Japan). Indirect immunofluorescence was performed using the following antibodies: goat anti-$p47^{phox}$ polyclonal antibody which recognized $p47^{phox}$, a cytosolic, regulatory subunit of NADPH oxidase (1:100 dilution; Abcam, Cambridge, MA, USA) and rabbit anti-Iba-1 polyclonal antibody (1:400; Wako Pure Chemical Industries Ltd, Osaka, Japan). Cells were incubated in primary antibodies diluted in PBS containing 5% normal horse serum at 4 °C overnight. After rinsing twice with PBS for 5 min, anti-goat rhodamine-conjugated secondary antibody (Southern Biotech, Birmingham, AL, USA) and anti-rabbit fluorescein isothiocyanate (FITC)-conjugated secondary antibody (Southern Biotech, Birmingham, AL, USA) were used for detection. Fluorescent images were captured with fluorescence microscope (OLYMPUS BX50; Olympus Co. Ltd, Tokyo, Japan).

2.7. Co-culture experiment with microglial and neuronal cell lines

The PC12 cells were plated on 24-well tissue culture plates at a density of 2×10^3 cells per 1 mL per well and were then incubated in the presence of 20 ng/mL nerve growth factor (NGF) at 37 °C for 7–10 days enough to develop neuritic formation. The 6-3 microglial cells were plated on Tissue Culture Inserts for 24-well plates (Greiner Bio-One GmbH, Frickenhausen, Germany) at a density of 1×10^5 cells per 200 μL per well and were then pre-incubated in the presence of DMSO (0.05%) or aripiprazole (10 μM) for 5 h and then each Tissue Culture Inserts was placed on the 24-well tissue culture plate with PC12 cells, respectively. After 2 h co-incubation with 400 ng/mL PMA, Tissue Culture Inserts were removed from the 24-well plates with PC12 cells. Neuritic beading formations of PC12 cells were observed and assessed under a phase-contrast microscope as previously reported (Park et al., 1996; Takeuchi et al., 2005). More than 100 neurons in duplicate wells were assessed blindly in three independent trials. The ratio of the numbers of neuritic beading (beads) per one neuronal cell was calculated.

2.8. Statistics

Data were expressed as the means ± SEM and analyzed by a one-way analysis of variance (ANOVA) followed by Tukey's post hoc test. The significance was established at a level of $p<0.05$. All the data of each group were confirmed to be normally distributed by the Shapiro–Wilk test ($p>0.05$).

3. Results

3.1. Effects of the antipsychotics on the $\cdot O_2^-$ production by PMA-stimulated microglia

First of all, we directly measured the generation of $\cdot O_2^-$ associated with PMA-stimulated murine 6-3 microglia by ESR spectroscopy with a spin trap DEPMPO. In the preparations of non-stimulated microglia (Fig. 1A), no signals were obtained. Microglial cells stimulated by 400 ng/mL PMA in the presence of DEPMPO showed prominent signals whose spectra consisted of a linear combination of a characteristic 12-line spectrum corresponding to $\cdot O_2^-$ spin adduct DEPMPO–OOH and an 8-line spectrum corresponding to OH spin adduct DEPMPO–OH (Fig. 1B). Computer simulation confirmed DEPMPO–OOH with hyper-fine splittings $a_N = 13.15$ G, $a^b_H = 10{:}59$ G, $a_p = 49.73$ G, $a^g_H = 0{:}72$ G and DEPMPO–OH with hyper-fine splittings $a_N = 12.43$ G, $a_H = 13.49$ G, $a_p = 50.39$ G. These values are consistent with those described previously (Sankarapandi et al., 1998). Previously, we had demonstrated that the spin adducts originated from $\cdot O_2^-$ radical, but not •OH− radical, which is derived from H_2O_2 (Hashioka et al., 2007b). In the present study, the effects of various types of antipsychotics on the generation of $\cdot O_2^-$ from PMA-stimulated microglia were evaluated. Pretreatment with aripiprazole, a partial D2R agonist, for 5 h considerably inhibited the signal intensity of the $\cdot O_2^-$ adduct (Fig. 1C), while other antipsychotics with D2R antagonism including haloperidol, olanzapine, clozapine and risperidone did not have any inhibitory effect on the signal intensity of the $\cdot O_2^-$ adduct (Fig. 1D–G). In order to confirm whether the inhibitory effect of aripiprazole was due to D2R agonism or not, the effect of quinpirole which is a D2R full agonist was evaluated. Quinpirole did not have any inhibitory effect on the signal intensity of the $\cdot O_2^-$ adduct (Fig. 1H). These results thus suggested that the inhibitory effects of aripiprazole on the generation of $\cdot O_2^-$ from PMA-stimulated microglia were independent of the effects of aripiprazole on D2R. In addition, we also prepared rat primary microglial cells for ESR to confirm the relevance of our results in the 6-3 cells. In the case of PMA-stimulated rat primary microglial cells, the $\cdot O_2^-$ like adduct was measured despite a very low signal intensity due to much smaller quantity of the rat primary microglial cells (1.6×10^4) than that of the 6-3 cells (1.6×10^6) (Fig. 2B). Aripiprazole considerably reduced the signal intensity of the above-mentioned $\cdot O_2^-$ like adduct (Fig. 2C). These results suggest that the inhibitory effects of aripiprazole on microglial activation were not limited to the 6-3 microglia. To confirm whether or not aripiprazole per se scavenges $\cdot O_2^-$, we measured the $\cdot O_2^-$ production in xanthine/xanthine oxidase system in both the presence and absence of aripiprazole by ESR monitoring with a spin trap DEPMPO. Fig. 3A shows typical ESR spectra consisting of DEPMPO–OOH and DEPMPO–OH in xanthine/xanthine oxidase system. The formation of these spin adducts via trapping $\cdot O_2^-$ was confirmed by our previous report (Hashioka et al., 2007b). The ESR spectra in the presence of aripiprazole (Fig. 3B) proved to be essentially the same as those shown in Fig. 3A, thus indicating that aripiprazole does not have scavenging effect on $\cdot O_2^-$. Similarly, other antipsychotics did not show any scavenging effect of $\cdot O_2^-$ (data not shown).

Since assays of free-radical production in cells are notoriously capricious (Abramov et al., 2005), in order to reinforce the ESR evidence above, we also quantified $\cdot O_2^-$ generation by the NBT assay. We observed that application of PMA significantly induced $\cdot O_2^-$ release from both the rat primary microglial cells (Fig. 4A) and the 6-3 microglial cells (Fig. 4B). Pretreatment with aripiprazole for 5 h significantly inhibited the $\cdot O_2^-$ release from PMA-stimulated microglial cells in comparison to the positive control, however, pretreatment of haloperidol and quinpirole did not have any inhibitory effects at all (Fig. 4B). In addition, we confirmed that 2 h-pretreatment of aripiprazole also inhibited the $\cdot O_2^-$ release dose-dependently (Fig. 4C). These results thus confirmed the relevance of the ESR results.

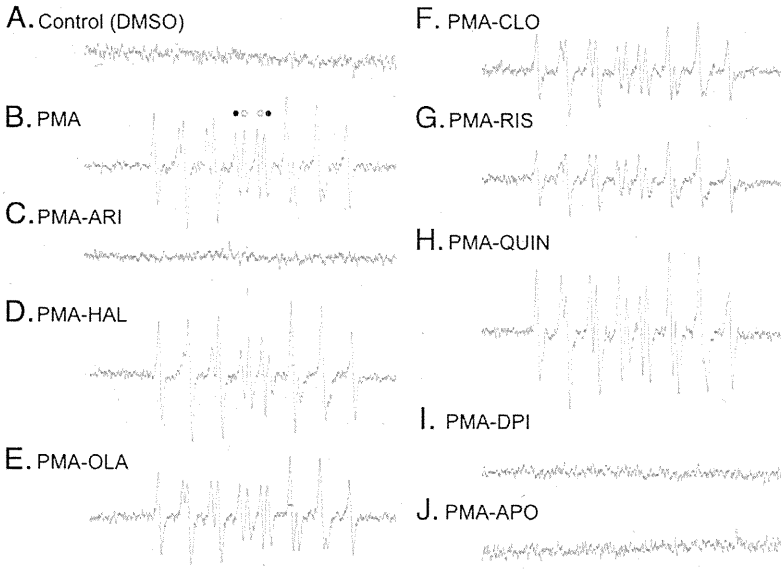

Fig. 1. Detection of $\cdot O_2^-$ generation by PMA-stimulated 6-3 microglial cells using ESR spin trap technique with DEPMPO. Murine 6-3 microglial cells (4×10^6/mL) were prepared and incubated with PMA (400 ng/mL) for 30 min at 37 °C with and without pretreatment of antipsychotics for 5 h. The ESR spectra were then recorded in the presence of 25 mM DEPMPO at room temperature. (A) ESR spectra of DEPMPO adducts obtained from non-stimulated microglia. (B) ESR spectra of DEPMPO adducts obtained from PMA-stimulated microglia. Open and closed circles represent measured signal peaks of DEPMPO–OH and DEPMPO–OOH adducts, respectively. (C) ESR spectra of DEPMPO adducts obtained from microglia stimulated by PMA (400 ng/mL) after a 5 h pretreatment with aripiprazole (10 μM). (D) The same as (C) but with haloperidol (10 μM). (E) The same as (C) but with olanzapine (10 μM). (F) The same as (C) but with clozapine (10 μM). (G) The same as (C) but with risperidone (10 μM). (H) The same as (C) but with quinpirole (10 μM). (I) The same as (C) but with DPI (10 μM). (J) The same as (C) but with apocynin (1 μM).

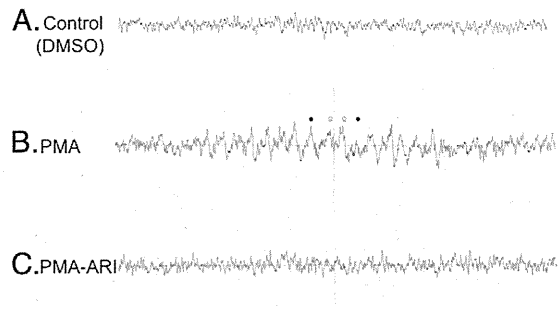

Fig. 2. Detection of $\cdot O_2^-$ generation by PMA-activated rat primary microglial cells using ESR spin trap technique with DEPMPO. Rat primary microglial cells (4×10^4/mL) were prepared and incubated with PMA (400 ng/mL) for 30 min at 37 °C with and without pretreatment of aripiprazole for 5 h. The ESR spectra were then recorded in the presence of 25 mM DEPMPO at room temperature. (A) ESR spectra of DEPMPO adducts obtained from non-stimulated microglia. (B) ESR spectra of DEPMPO adducts obtained from PMA-stimulated microglia. Open and closed circles represent measured signal peaks of DEPMPO–OH and DEPMPO–OOH adducts, respectively. (C) ESR spectra of DEPMPO adducts obtained from microglia stimulated by PMA (400 ng/mL) after a 5 h pretreatment with aripiprazole (10 μM).

3.2. Aripiprazole inhibits PMA-induced translocation of NADPH oxidase cytosolic subunit of PHOX p47^{phox} to the plasma/phagosomal membranes

In the ESR experiments, not only aripiprazole but also NADPH oxidase inhibitors (diphenylene iodonium (DPI) and apocynin) proved to have a considerable inhibitory effect on PMA-induced $\cdot O_2^-$ generation from the murine microglial cells (Fig. 1I and J). Therefore, our results suggest that the $\cdot O_2^-$ generation in the microglial cells depends on NADPH oxidase pathway as previously reported (Sankarapandi et al., 1998). Inhibitory process of NADPH oxidase is reported to be different between DPI and apocynin: apocynin inhibits the translocation of subunits such as p47 and p67 in cytosol, while DPI acts by abstracting an electron from an electron transporter and forming a radical, which then inhibits the respective electron transporter through a covalent binding step in membrane (Bedard and Krause, 2007).

In the DMSO treatment group, the 6-3 cells showed typical resting morphology with small cell bodies (Fig. 5A). On the other hand, PMA-

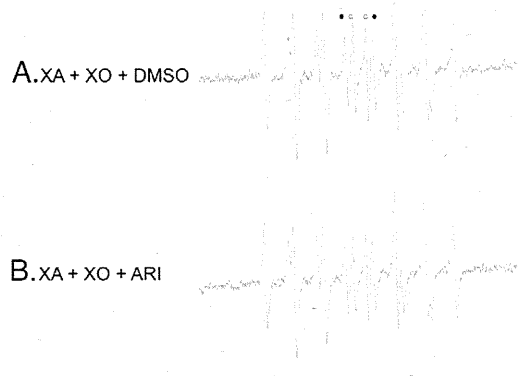

Fig. 3. Detection of $\cdot O_2^-$ generation in xanthine/xanthine oxidase system using ESR spin trap technique with DEPMPO. The system contained 0.4 mM xanthine, 2 mM DTPA, and 20 mM DEPMPO in PB in the presence and absence of 10 μM aripiprazole. Xanthine oxidase (0.1 U/mL) was added last to the mixture to start the reaction. (A) ESR spectra of DEPMPO adducts obtained in the xanthine/xanthine oxidase system in the presence of the control DMSO (final concentration: 0.05%). Open and closed circles represent measured signal peaks of DEPMPO–OH and DEPMPO–OOH adducts, respectively. (B) The same as (A), but also in the presence of aripiprazole (10 μM).

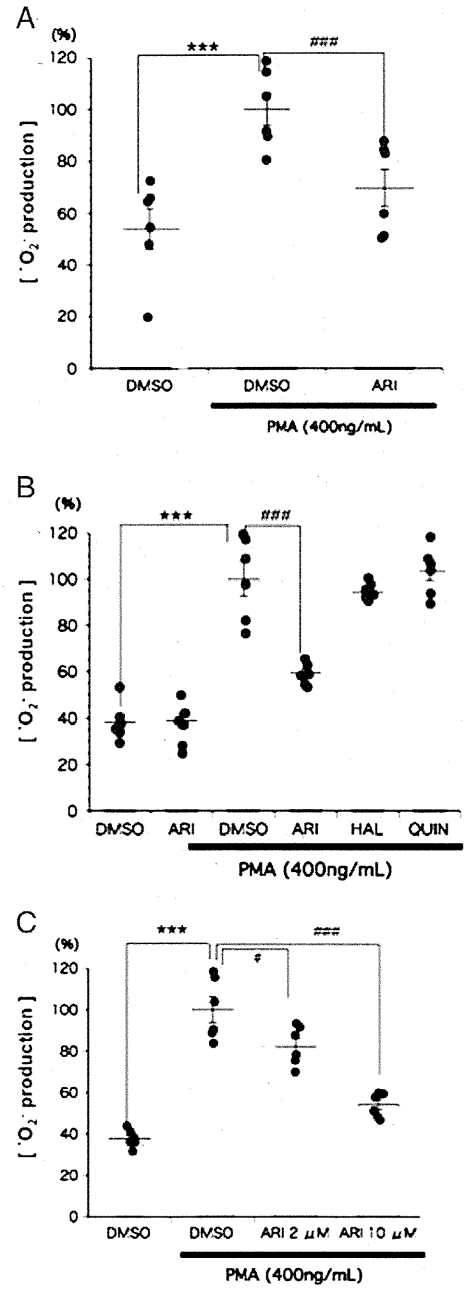

Fig. 4. Quantification of $\cdot O_2^-$ production in microglial cells by Nitro blue tetrazolium (NBT) assay. (A) The rat primary microglial cells were pre-treated with DMSO (0.05%) and aripiprazole (10 μM) for 5 h, then the cells were treated with PMA (400 ng/mL) for 30 min. The $\cdot O_2^-$ production was determined using the NBT assay. The results were expressed as percentage values taking the PMA + DMSO treatment group as 100%. (B) The mouse 6-3 microglial cells were pre-treated with DMSO (0.05%), aripiprazole (10 μM), haloperidol (10 μM) and quinpirole (10 μM) for 5 h, then the cells were treated with PMA (400 ng/mL) for 30 min. The $\cdot O_2^-$ production was determined using the NBT assay. The results were expressed as percentage values taking the PMA + DMSO treatment group as 100%. All data are represented as the means (SEM) of three independent experiments (n = 6–9). ***P<0.001 in comparison to the control DMSO treatment group. ###P<0.001 in comparison to the PMA + DMSO treatment group. (C) The mouse 6-3 microglial cells were pre-treated with DMSO (0.05%) and aripiprazole (10 μM) for 2 h, then the cells were treated with PMA (400 ng/mL) for 30 min. The $\cdot O_2^-$ production was determined using the NBT assay. The results were expressed as percentage values taking the PMA + DMSO treatment group as 100%. All data are represented as the means (SEM) of three independent experiments (n = 6–9). ***P<0.001 in comparison to the control DMSO treatment group. #P<0.05/###P<0.001 in comparison to the PMA + DMSO treatment group.

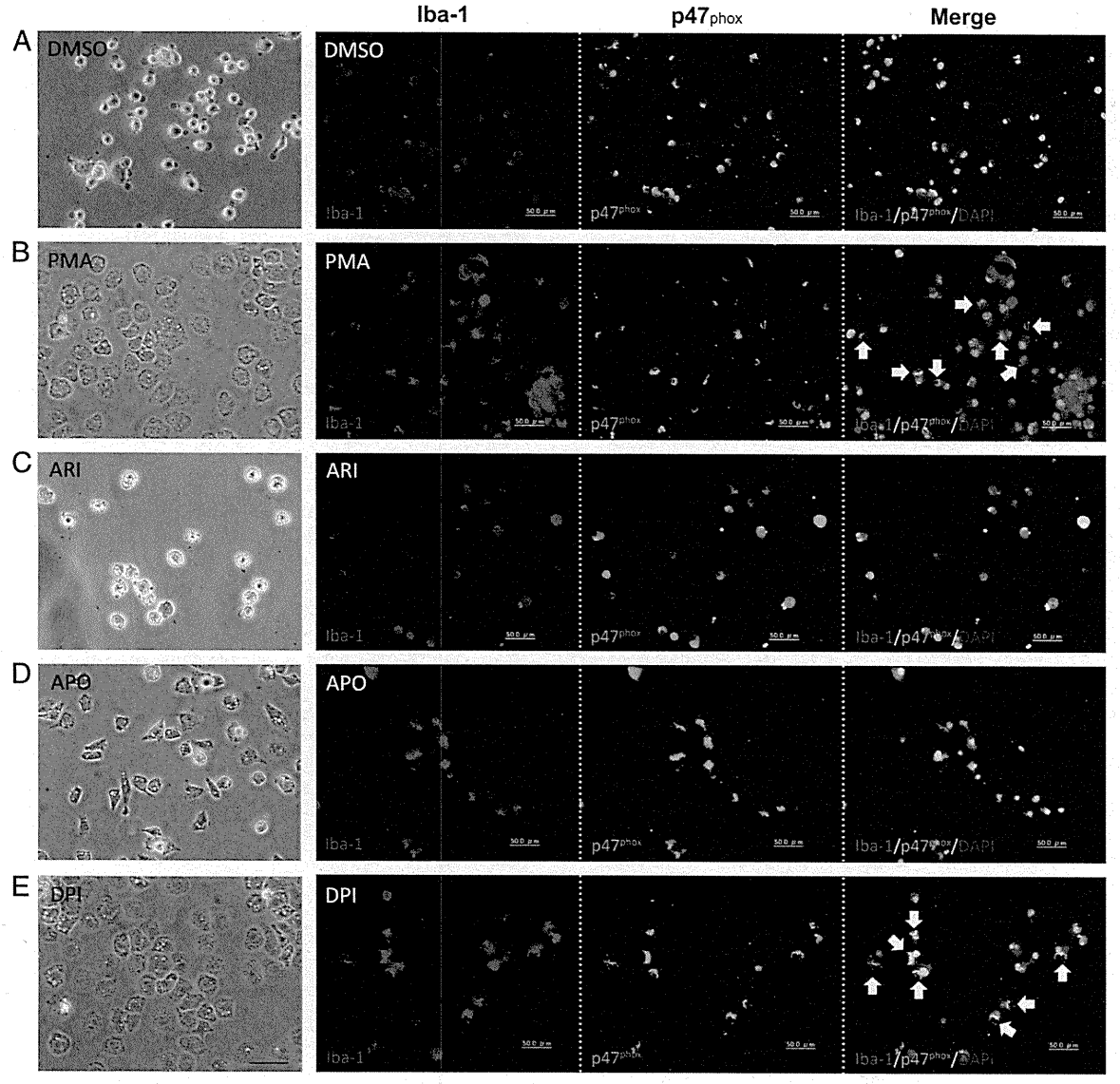

Fig. 5. Microglial cell morphology and cytosolic p47^{phox} protein translocation. Cell morphology of the murine 6-3 microglia is shown in the leftmost line, and the existence of cytosolic Iba-1 (red), p47^{phox} (green) and nuclear (DAPI; blue) is shown in the second-leftmost line, second-rightmost line and rightmost line, respectively. In the absence of PMA, cells showed resting shapes and p47^{phox} was localized in the cytosol (A). Both PMA-treatment cells and DPI-pretreatment cells showed ameboid shapes and p47^{phox} was translocated to the plasma/phagosomal membranes, especially phagosomal membranes inside the cytosol with a ring structure (arrows) (B and E). Both aripiprazole- and apocynin-pretreatment cells showed spindle shapes and p47^{phox} was localized in the cytosol without ring structures (C and D). Scale bar indicates 50 μm.

treated 6-3 cells underwent ameboid shapes with cytoplasmic vacuoles (Fig. 5B). DPI-pretreated cells were also changed to ameboid shape morphology after PMA-stimulation (Fig. 5D). Aripiprazole- or apocynin-pretreated cells followed by PMA-stimulation were exhibited in various types of morphology, including roundish and multipolar spindle shapes (Fig. 5C and E).

Activation of NADPH oxidase has been reported to require phosphorylation and subsequent translocation of the cytosolic component p47^{phox}, together with other NADPH oxidase cytoplasmic subunits to the plasma membrane and/or the phagosomal membranes in the cytoplasm (Bedard and Krause, 2007; Liva et al., 1999). As aripiprazole considerably inhibits $\bullet O_2^-$ production induced by PMA, we sought to determine whether aripiprazole inhibits NADPH oxidase activation by preventing the translocation of p47^{phox} from the cytosol to the membranes after PMA stimulation. Immunostaining for the p47^{phox} demonstrated that cytosolic p47^{phox} was formed ring-like structure after PMA treatment in the cytoplasm (Fig. 5B), suggesting that phosphorylated p47^{phox} was mainly translocated to the phagosomal membranes. Aripiprazole- or apocynin-preincubated cells were prevented this formation (Fig. 5C and D). In DPI-pretreated cells, p47^{phox} was also formed ring-like structure as well as PMA-treated cells (Fig. 5E). In cells treated with DMSO alone in the absence of PMA stimulation, p47^{phox} remained localized primarily in the cytosol (Fig. 5A).

Therefore, one mechanism by which aripiprazole inhibits $\bullet O_2^-$ production in microglial cells seems to be through the inhibition of p47^{phox} translocation to the membranes after PMA stimulation, which is similar to the inhibitory process of apocynin.

3.3. Aripiprazole attenuates the mobilization of intracellular Ca^{2+} induced by PMA in microglia

Next, we investigated the effect of aripiprazole on the mobilization of intracellular Ca^{2+} induced by PMA in rat primary microglia. PMA are known to induce $\cdot O_2^-$ from microglia with the elevation of intracellular Ca^{2+} (Colton et al., 1992; Yoo et al., 1996). In the present study, we observed that PMA (400 ng/mL) acutely induced a transient increase in $[Ca^{2+}]i$ in the rat primary microglia (n = 50 cells; Fig. 6A and C), as previously reported in human microglia (Yoo et al., 1996). Pretreatment of 5 μM aripiprazole for 5 h attenuated the PMA-induced increase in $[Ca^{2+}]i$ (n = 18 cells; Fig. 6B and C). Pretreatment of 1 μM apocynin also attenuated the PMA-induced increase in $[Ca^{2+}]i$ (n = 5 cells; Fig. 6C), while pretreatment of 10 μM DPI did not affect the PMA-induced increase in $[Ca^{2+}]i$ in the rat microglial cells (n = 29 cells; Fig. 6C).

3.4. Aripiprazole attenuates the production of neuritic beading induced by activated microglia

Finally, neuronal damage induced by microglial activation was investigated with the co-culture experiment. Presence of neuritic bead is one of the earliest outcomes of neuronal damage (Park et al., 1996; Takeuchi et al., 2005). PMA-treatment with 6-3 microglial cells for 2 h obviously induced neuritic beading of PC12 cells (Fig. 7A, B and D). Pretreatment of aripiprazole for 5 h significantly reduced the formation of neuritic beading (Fig. 7C and D). Our results indicate that aripiprazole protected from formation of neuritic beading induced by PMA-stimulated microglial activation.

4. Discussion

This is the first report to demonstrate that among typical and atypical antipsychotics, only aripiprazole inhibited the generation of $\cdot O_2^-$ from PMA-stimulated microglia. Aripiprazole proved to inhibit the generation of $\cdot O_2^-$ through the cascade of PKC activation, intracellular Ca^{2+} regulation and NADPH oxidase activation in microglial cells. In addition, aripiprazole indicated to have neuroprotective effects via inhibiting microglial activation by the co-culture experiment.

The typical dose range of aripiprazole is 10–30 mg/day and the typical serum concentration or plasma range of aripiprazole is 0–1000 ng/mL (0–2 μM) (Alexopoulos et al., 2004; Chew et al., 2006; Grunder et al., 2008). Antipsychotics are known to accumulate in brain tissue to levels that are 25–30 fold higher than serum levels (Baumann et al., 2004). Therefore, in spite of no evidence that the effect of a drug in cell culture could be compared to the effect of the same drug at a brain tissue level even in the same range of concentration, the concentrations of aripiprazole used in the present study might thus not be substantially different from the brain tissue levels for aripiprazole. The same concentrations were applied to other antipsychotics (haloperidol, olanzapine, clozapine and risperidone) according to previously published in vitro studies using microglial cells (Hou et al., 2006; Kato et al., 2007, 2008).

Aripiprazole is a high-affinity D2R partial agonist, while other antipsychotics investigated in the present study are all D2R antagonists (Burris et al., 2002; Shapiro et al., 2003). These differences may be relevant to the results shown in the present study. Farber et al. provided the first evidence of the existence of functional dopamine receptors on microglia. In their study, quinpirole inhibited the release of NO from LPS-induced microglia dose-dependently (Farber et al., 2005). On the other hand, in our previous study, not quinpirole but aripiprazole showed inhibitory effects on the generation of NO and TNF-α from interferon-γ-stimulated microglia (Kato et al., 2008). Moreover, in the present study, quinpirole did not have any inhibitory effects on the generation of $\cdot O_2^-$ from PMA-stimulated microglia. These results seem to suggest that the dopamine D_2 receptors may not be involved in the generation of $\cdot O_2^-$ from PMA-stimulated microglia and in the inhibition of $\cdot O_2^-$ production by aripiprazole shown in the present study. Aripiprazole has affinities of other receptors such as

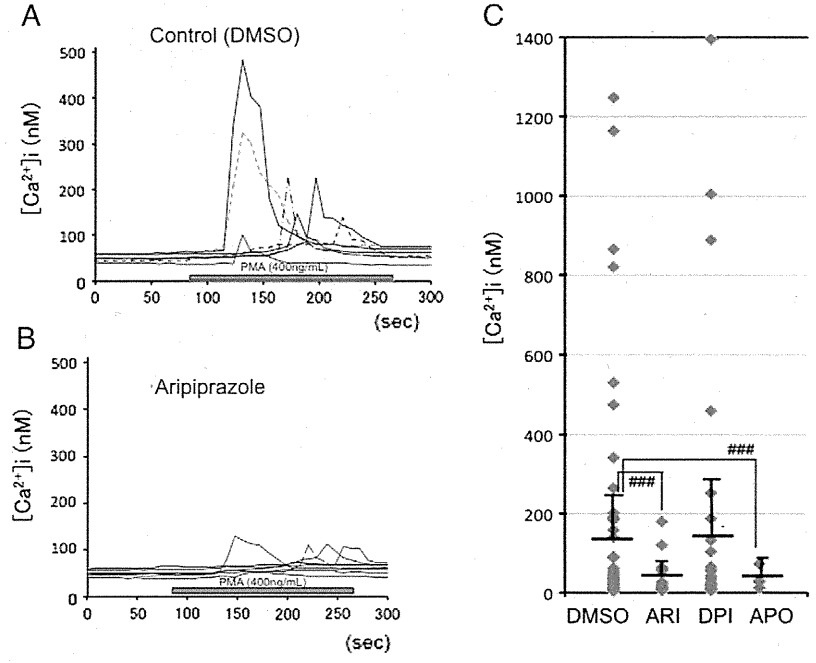

Fig. 6. Aripiprazole attenuates the mobilization of intracellular Ca^{2+} induced by PMA in rat microglia. (A and B) Seven representative traces showing a brief application (3 min) of 400 ng/mL PMA induced a transient increase in $[Ca^{2+}]i$ in rat microglia pretreated with DMSO (0.025%; in A) and with aripiprazole (5 μM; in B). (C) Bar graph summarizing the effect of different manipulations on the peak amplitude of PMA-induced increase in $[Ca^{2+}]i$ in rat microglia. Increase of $[Ca^{2+}]i$ in response to PMA application with DMSO, aripiprazole, DPI and apocynin was calculated as a difference between basal $[Ca^{2+}]i$ and highest $[Ca^{2+}]i$ during the treatment of PMA, respectively. All data presented were obtained from at least five dishes and three different cell preparations. Data are expressed as the mean ± SEM. ###P<0.001 in comparison to the PMA + DMSO treatment group.

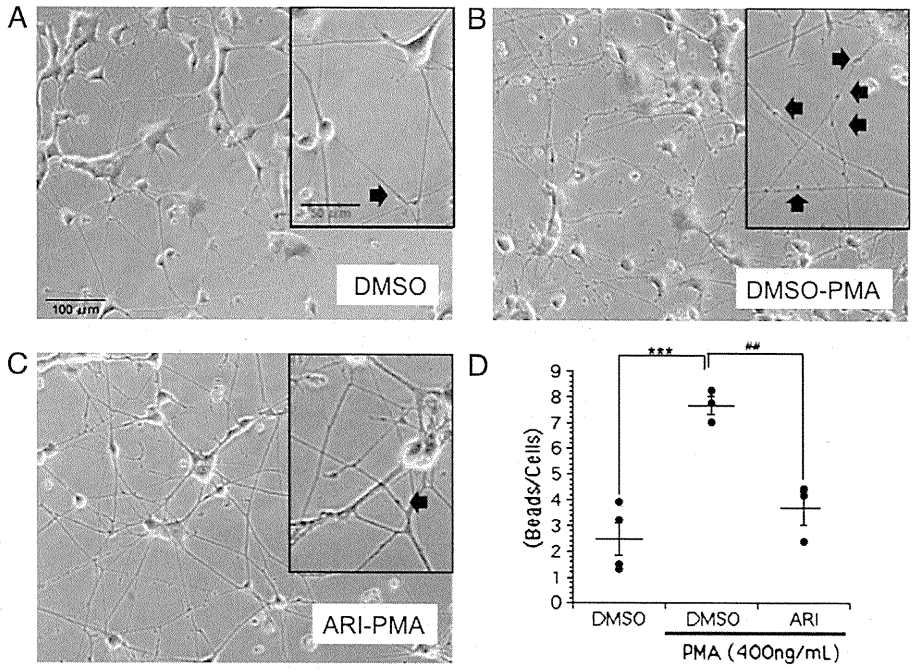

Fig. 7. Neuritic beading induced by PMA-stimulated microglia. Neuritic formation of the PC12 cells, which was taken under a phase-contrast microscope, is shown in the main photo and enhanced photo is shown in the upper right-hand corner (enhanced) (A–C). (A) Pretreatment with DMSO (0.05%), following co-culture with the 6-3 microglial cells without PMA treatment for 2 h. (B) Pretreatment with DMSO (0.05%), following co-culture with the 6-3 microglial cells with 400 ng/mL PMA treatment for 2 h. (C) Pretreatment with aripiprazole (10 μM), following co-culture with the 6-3 microglial cells with 400 ng/mL PMA treatment for 2 h. (D) Quantification of neuritic beading. The number of neuritic beading (beads) under more than 100 neuronal cell bodies was assessed blindly in three independent trials. All data are expressed the means (SEM) of the number of neuritic beading (beads) per one neuronal cell (each: 3–4 trials). ***P<0.001 in comparison to the control DMSO treatment group. ##P<0.01 in comparison to the DMSO + PMA treatment group.

serotonin (Shapiro et al., 2003). Our recent study has proved that not only antipsychotics but also antidepressants have inhibitory effects of microglial activation (Horikawa et al., 2010), which indicate that other pharmacological mechanism beyond D2R may exist in our findings. Further investigation is required in order to clarify the underlying mechanism.

We showed the first evidence that aripiprazole attenuates the mobilization of intracellular Ca^{2+} induced by PMA in rat microglia. PMA is known to induce $\bullet O_2^-$ from microglia with the elevation of intracellular Ca^{2+} (Colton et al., 1992; Yoo et al., 1996). Intracellular Ca^{2+} is one of the endogenous activators of PKC. Regarding mammalian astrocytes, PMA proved to activate the NADPH oxidase through the activation of PKC, while the elevation of intracellular Ca^{2+} induced by PMA itself activates the NADPH oxidase independently of PKC (Abramov et al., 2005). We showed that aripiprazole inhibits NADPH oxidase activation by preventing the translocation of $p47^{phox}$ from the cytosol to the membrane after PMA stimulation. Our results suggest that the $\bullet O_2^-$ generation in the microglial cells depends on NADPH oxidase pathway, inhibitory effects of which are similar not to DPI but to apocynin. Summing up these results, aripiprazole indicates to inhibit the $\bullet O_2^-$ generation through the NADPH oxidase by suppressing the elevation of intracellular Ca^{2+} in PMA-treated microglia.

Antioxidants have recently been regarded to have protective effects in neurodegeneration, and microglial activation via NADPH oxidase has a key role in this process (Wang et al., 2006). NADPH-derived ROS such as $\bullet O_2^-$ and •OH radicals have been reported not only to cause microglial proliferation but also to amplify the proinflammatory gene expressions, both of which are associated with neurotoxicity induced by activated microglia (Pawate et al., 2004; Qin et al., 2004). In our previous study, risperidone and other atypical antipsychotics with D2R antagonism inhibited the production of proinflammatory cytokines (Bian et al., 2008; Kato et al., 2007), however these antipsychotics have no inhibitory effect of releasing $\bullet O_2^-$ radicals from activated microglia in the present study. On the other hand, aripiprazole proved to have dual inhibitory effects of releasing pro-inflammatory cytokines (Kato et al., 2008) and $\bullet O_2^-$ radicals from activated microglia in the present study. Therefore, we presume aripiprazole to be the strongest antioxidative/anti-inflammatory agent among antipsychotics.

We previously demonstrated that aripiprazole inhibits microglial activation induced by IFN-γ and suggested that this inhibitory effect is related to the inhibition of the cell signaling pathways including PKC, p38MAPK, and ERK (Kato et al., 2008). PMA is a PKC activator and PKC pathway is located in the upstream of both p38MAPK and ERK pathways in the process of PMA-induced microglial activation as shown in Nikodemova et al. (2006). Therefore, the inhibitory effects of aripiprazole on neuritic beading which was shown in the present co-culture study is probably due to the inhibitory effects of aripiprazole on the generation of both $\bullet O_2^-$ and pro-inflammatory cytokines from PMA-stimulated microglia.

Structural brain abnormalities such as progressive gray matter loss have been extensively and consistently described in schizophrenic patients (Davis et al., 2003; Kumra et al., 2005). This evidence is the primarily propounded mechanism explaining the neurodegenerative course of schizophrenia (Salisbury et al., 2007). Multiple lines of evidence combine to implicate the increased susceptibility to apoptotic death in the pathophysiology of schizophrenia (Glantz et al., 2006). The activation of apoptotic process can lead to a rapid neuronal death (Glantz et al., 2006; Jarskog et al., 2005). Microglial NADPH oxidase pathway has recently been reported to play a key role in the process of neuronal deaths (Qin et al., 2006). Furthermore, our results of co-culture experiment suggest that activation of microglial NADPH oxidase pathway induces neuritic beading formation, which is one of the initial steps of neuronal damage (Park et al., 1996; Takeuchi et al., 2005). In addition, aripiprazole attenuated the neuritic beading formation, which indicates that aripiprazole may be a neuroprotective agent via inhibiting microglial activation. One recent animal study